Gravitational back-reaction is magical

ChunJun Cao, a,b Gong Cheng, b Alioscia Hamma, c,d,e Lorenzo Leone, b William Munizzi, b Savatore F.E. Oliviero b

- ^a Institute for Quantum Information and Matter, California Institute of Technology, Pasadena, CA 91125. USA
- ^bDepartment of Physics, Virginia Tech, Blacksburg, VA 24061, USA
- ^cDipartimento di Fisica 'Ettore Pancini', Università degli Studi di Napoli Federico II, Via Cintia 80126, Napoli, Italy
- ^dINFN, Sezione di Napoli, Italy
- ^eScuola Superiore Meridionale, Largo S. Marcellino 10, 80138 Napoli, Italy
- ⁹ Dahlem Center for Complex Quantum Systems, Freie Universität Berlin, 14195 Berlin, Germany
- ^hDepartment of Physics, Arizona State University, Tempe, AZ 85281, USA
- ⁱ NEST, Scuola Normale Superiore and Istituto Nanoscienze, Consiglio Nazionale delle Ricerche, Piazza dei Cavalieri 7, IT-56126 Pisa, Italy

E-mail: cjcao@vt.edu, gongc@vt.edu, alioscia.hamma@unina.it, lorenzo.leone@fu-berlin.de, wmunizzi@asu.edu, salvat.oliviero@sns.it

ABSTRACT: We study the interplay between magic and entanglement in quantum many-body systems. We show that non-local magic, which is supported by the quantum correlations is lower bounded by the non-flatness of entanglement spectrum and upper bounded by the amount of entanglement in the system. We then argue that a smoothed version of non-local magic bounds the hardness of classical simulations for incompressible states. In conformal field theories, we conjecture that the non-local magic should scale linearly with entanglement entropy but sublinearly when an approximation of the state is allowed. We support the conjectures using both analytical arguments based on unitary distillation and numerical data from an Ising CFT. If the CFT has a holographic dual, then we prove that the non-local magic vanishes if and only if there is no gravitational back-reaction. Furthermore, we show that non-local magic is approximately equal to the rate of change of the minimal surface area in response to the change of cosmic brane tension in the bulk.

Contents

1	Introduction	1
2	Main results	2
	2.1 Quantum information-theoretic results	4
	2.2 AdS/CFT results	5
3	Non-local Magic	5
	3.1 Magic measures	5
	3.2 (Anti-)Flatness	S
	3.3 Non-local Magic, Entropy, and anti-Flatness	13
	3.3.1 Non-local magic and flatness	13
	3.3.2 Non-local stabilizer relative entropies of magic	14
	3.3.3 Magic estimates	15
	3.3.4 Smoothed magic	16
4	Magic in conformal field theories	18
	4.1 Geometric Interpretation through tensor networks	18
	4.2 Non-local magic in Ising model	23
	4.3 Smoothed Magic from Entropic Bounds	26
5	Holographic Magic and Gravity	29
	5.1 Brane tension and magic	30
	5.2 Magic in Holographic CFT	31
6	Discussion	36
\mathbf{A}	Invariance of $STAB_0$	39
	A.1 Prof of Proposition 3	40
В	Proof of Theorem 1	41
\mathbf{C}	Stabilizer relative entropies	43
	C.1 Proof of Theorem 2	43
	C.2 Proof of Proposition 5	44
	C.3 Proof of Theorem 4	45
D	Estimate by Stabilizer-Rényi-entropy	46
	D.1 Proof of Theorem 3	46
	D.2 Proof of Proposition 8	48
	D.3 Distillation of Matrix Product State	49

\mathbf{E}	Validity of various bound for magic	51
\mathbf{F}	Supplemental results for Ising Model	52
	F.1 Symmetry breaking phase	52

1 Introduction

Entanglement is an important quantum resource and an integral part of our understanding of quantum many-body physics and quantum gravity, such as topological order [1–3], non-equilibrium dynamics [4–7], spacetime [8], and black holes [9, 10]. In the Anti-de Sitter/Conformal Field Theory (AdS/CFT) correspondence [11, 12], entanglement in the CFT is important for emerging spacetime geometry [13–17] in the dual gravity theory, e.g. via the Ryu-Takayanagi formula[18–21]. Surprisingly, this connection between geometry and entanglement holds not only for holographic CFTs, but also for more general quantum many-body systems like tensor network toy models, which have been enormously successful in reproducing an analogous Ryu-Takayanagi formula[22], the emergent bulk geometry, and subregion operator reconstruction through quantum error correction[23–28]. This is a profound development as it suggests the lessons from holography may also apply beyond the confines of AdS[29–31].

However, the entanglement patterns in the tensor network models alone do not capture the full quantum landscape spanned by holography. Despite many recent advances[27, 32–36], it is still unclear how gravity can emerge in such models. In particular, neither the holographic stabilizer codes[23] nor the random tensor networks[24] can fully capture the CFT entanglement spectrum and gravitational back-reaction. Stabilizer tensor networks also fail to capture power-law correlations, robust multi-partite entanglement, and non-trivial area operators[37–39]. From a resource-theoretic perspective, what are these tensor network models missing compared to the low energy states in holographic theories? We show in this work that the answer is magic[40–43], or more precisely, non-local magic.

Quantumness comes in two layers: entanglement gives the power of building correlations stronger than classical and violates Bell's inequalities while quantum advantage characterizes the hardness of simulating quantum systems on a classical computer. The latter is distinct from entanglement — a task involving a highly entangled system is not always hard to simulate classically as it can be achieved purely using Clifford operations that are classically simulable. This notion of classical hardness that constitutes the second layer of quantumness is intimately connected to the amount of non-stabilizerness, also known as magic, in the system. Although magic alone cannot generate the intricate patterns of complexity that are crucial for the complex behavior in a quantum wave-function, when used in conjunction with Clifford operations, non-stabilizerness [40] is both necessary and sufficient in realizing (fault-tolerant) universal quantum computation. Therefore, it is the remaining piece needed for quantum advantage and for simulating holographic conformal field theories.

In addition to being an important resource for fault-tolerant quantum computation [40, 41] and quantum simulation, pioneering work has established magic as an important ingredient for characterizing quantum many-body systems [44–47], such as dynamics [42, 48–50], quantum phases [51, 52], quantum circuits [53–55], and randomness [56]. In the context of holography, [44, 47, 57] showed that magic is abundant in CFTs and is therefore expected to play an important role for reproducing the correct CFT entanglement spectrum, for generating power-law correlations, for building non-trivial area operators in holographic codes, and for reproducing the correct multipartite entanglement in holographic geometries [38].

There are also many questions surrounding the role played by magic. Empirically, the amount of non-stabilizerness or non-Gaussianity [41, 43, 59–64] present in a quantum process appears to correlate with the hardness of classical simulations [65], e.g. in stabilizer and matchgate simulations [66–72] as well as in Monte Carlo sampling [73]. However, its precise connection with complexity is yet unclear. While it is proposed [39, 44] that the replication of the CFT entanglement spectrum and emergent gravity in AdS/CFT requires magic, the specific mechanism through which magic accomplishes this also remains uncertain. Furthermore, although the amount of magic present in a system can be illuminating all by itself, it is becoming clear the distribution of magic is equally, if not more, important for understanding non-equilibrium dynamics and entanglement spectrum [74]. For example, the amount of magic is generally expected to scale volumetrically with the number of qubits in quantum many-body systems. The tensor product of nonstabilizer states, CFT ground states, and Haar random states all have a high magic density and volume law magic scaling, and yet their physical properties and their usefulness for quantum computation are completely different. Therefore, a more profound understanding of the interplay between entanglement and magic will shed new light on the structure of quantum matter, quantum information, and gravity.

In this work, we report multiple advances in respond to the above queries. We define non-local magic and offer compelling evidence for how it is connected to the hardness in classically simulating incompressible states. We provide rigorous bounds as well as computable estimates for non-local magic in any quantum system and show that it is lower bounded by the anti-flatness of the entanglement spectrum and upper bounded by various functions of the Rényi entropies. When applied to CFTs, we propose a straightforward relationship between magic, entropy, and anti-flatness. For theories with holographic dual, we show that the non-local magic controls the amount of gravitational back-reaction in response to stress energy, and thus critical for the emergence of gravity.

2 Main results

In this section, we explain the main results of this paper and lay down informally the setup and strategy of this work. Then, in the following sections, we derive them rigorously. The main goal of this paper is to show that the non-local magic is responsible for the non-flat

¹Although this is not noted by the authors explicitly, it is clear that holographic states require $O(1/G_N)$ tripartite entanglement but cannot be predominantly GHZ-type[58].

entanglement spectrum in a CFT and for the back-reaction in AdS through the AdS-CFT dictionary.

Since the seminal work of Ryu and Takayanagi [18], a number of entries have been added to the AdS-CFT dictionary where one can connect quantum information theoretic quantities on the boundary to geometric quantities in the bulk. Notably, the correspondence can be used to find the holographic dual to functions of the spectrum of a reduced density operator ψ_A in the conformal field theory[75], where A is a subsystem of the CFT. The strategy of this work is to find a holographic dual of magic in a state ψ by connecting it to the spectrum of its reduced density operator ψ_A .

At the first sight, this may seem like an impossible task. There are two reasons: first of all, the way magic relates to spectral properties is complicated. The reason is that, as long as magic *only* quantifies the distillability of non-Clifford resources, convex combinations through a probability distribution p_i cannot create resources. However, we may think of magic in a way such that these probabilities are resourceful. In this case, there is a different resource theory of magic that we call STAB₀. This is the resource theory of magic established by the null set of stabilizer entropy[76]. We will first therefore first develop this theory by employing as monotones both the trace distance M_{dist} and relative entropy of resource M_R . They will both be useful later to establish our results.

The second reason why mapping magic in a spectral quantity is problematic is due to the fact that magic is generally a property of the full state ψ , which has trivial spectrum if pure. What has a non-trivial spectrum is the reduced state ψ_A to a subregion A, because of entanglement. Then the question becomes: how can the spectrum of ψ_A give us information on the magic of the full parent state ψ ?

The answer comes from the remarkable fact that the magic of a state ψ is related to the average deviation from the flat spectrum of the spectrum of the reduced density operator ψ_A through the Clifford orbit [74, 77]. The Clifford orbit preserves the magic, but entangles the system [78–80], therefore populating the spectrum of the reduced density operator. In fact, there is no need to take this average, as long as the spectrum of the subsystem density operator possesses an entropy obeying volume law. In this case, its flatness (or lack thereof) is enough to probe the magic of the full state.

Unfortunately, this is not good enough to explore CFT as these states are not hosting volume law for entanglement. In order to exploit the flatness-magic correspondence for a theory that generally has an area-law scaling of entanglement, we must focus on the boundary ∂A between the subregions A and its complement B where most of the entanglement is being mediated. On the Hilbert subspace supported on ∂A , the density operator $\psi_{\partial A}$ is well populated and as a consequence, we can compute its magic through the spectrum. This gives rise to the notion of non-local magic.

The main results of this work are grouped in two parts: (i) Quantum information-theoretic results that rigorously define non-local magic for both the magic measures defined above, namely the trace distance of non-local magic $M_{dist}^{(NL)}$ and the relative entropy of non-local magic $M_R^{(NL)}$ and relate them to spectral quantities. In particular, it will play an important role in the notion of anti-flatness $\mathcal{F}[74]$, that is, a measure of how much the

spectrum of a density operator is far from a flat distribution; and (ii) the application of these tools to AdS/CFT by first making precise the relation between entanglement, non-local magic and spectral flatness in a CFT. Then for holographic CFTs, we show that the holographic dual of gravitational back-reaction is indeed non-local magic.

2.1 Quantum information-theoretic results

The first result is that, given the bipartition AB, for a subsystem A of a quantum state ψ_{AB} , $M_{dist}^{(NL)}$ is lower bounded by the anti-flatness $\mathcal{F}(\psi_A)$ and upper bounded by the entanglement:

$$\mathcal{F}(\psi_A)/8 \le M_{dist}^{(NL)}(\psi_{AB}) \le \sqrt{1 - e^{-S_{max}(A)} + e^{S_{\infty}(A)} \left(1 - \frac{e^{\log d \lfloor S_{max}(A)/\log d \rfloor}}{e^{S_{max}(A)}}\right)}$$
(2.1)

where $\lfloor \cdot \rfloor$ is the floor function, $S_{max}(A) := \log \operatorname{rank} \psi_A$, $S_{\infty}(A) = \lambda_{\max}(\psi_A)$. For this, we assume the total Hilbert space is a tensor product of qubits (or qudits) with uniform local dimension d.

Second, by using the non-local magic measured by relative entropy $M_{RS}^{(NL)}$, one can find another relationship between magic in a quantum state ψ and its entanglement:

$$S_{max}(A) - S(A) \le M_{RS}^{(NL)}(\psi_{AB}) \le \log d \lceil S_{max}(A) / \log d \rceil, \tag{2.2}$$

where $\lceil \cdot \rceil$ is the ceiling function. The lower and upper bounds in the above equation are essentially tight for weakly-entangled states. Eq. (2.2) has also the advantage of allowing one to find good estimates for $M_{RS}^{(NL)}(\psi_{AB})$ in terms of the Schmidt coefficients of ψ_{AB} (see Eq. (3.52)). This is important because non-local magic is otherwise very difficult to calculate. Moreover, the relative entropy of magic allows us to define the smoothed (non-local) magic as

$$M_{RS}^{(NL,\epsilon)}(\psi_{AB}) := \min_{\|\chi - \psi_{AB}\| \le \epsilon} M_{RS}^{(NL)}(\chi).$$
 (2.3)

For a pure state therefore, we obtain the bounds

$$S_{max}^{\epsilon}(A) - (1 - \epsilon)^{-1} S(A) \le M_{RS}^{(NL,\epsilon)}(\psi_{AB}) \le \log d \lceil S_{max(A)}^{\epsilon} / \log d \rceil, \tag{2.4}$$

with the smoothed maximal entropy is defined as $S_{max}^{\epsilon}(A) := \min_{\|\chi - \psi_A\| < \epsilon} \ln(\operatorname{rank}(\chi))$. Since the lower bound quantifies the compressibility of a state, we show that incompressible states with low entanglement, but high non-local magic, can still be difficult to classically simulate.

Finally for a system of qubits, we use the spectral information $\{\lambda_i\}$ of state ψ , along with the magic measure known as stabilizer 2-Rényi entropy \mathcal{M}_2 , to estimate the non-local magic $\mathcal{M}_2(\{\lambda_i\})$. This calculation yields a tighter upper bound on non-local magic than Eq. (2.2), stating

$$\mathcal{M}_2^{NL}(\psi_{AB}) \le \min\{2S_2(A), 4(S_{max}(A) - S_{1/2}(A))\},$$
 (2.5)

where $S_n(A)$ are the Rényi-n entropies of ψ_A and S_{max} is the logarithm of Schmidt rank, which is taken to be an integer power of two.

For each of the above measures, we show that non-local magic vanishes if and only if the entanglement spectrum is flat, see Lemma 1.

2.2 AdS/CFT results

We now state the main holographic result of this work. One can use non-local magic to derive an RT-like formula for gravitational back-reaction, defined as the susceptibility of a backreacted surface area \mathcal{A} with respect to the insertion of a cosmic brane with tension \mathcal{T} . The first step is connecting back-reaction to spectral quantities. We obtain,

$$\frac{\partial \mathcal{A}}{\partial \mathcal{T}}\Big|_{\mathcal{T}=0} \approx -\left(\frac{4G}{\operatorname{Pur}(\psi_A)}\right)^2 \mathcal{F}(\psi_A),$$
 (2.6)

where the approximation holds when $S_2(A) - S_3(\psi_A) < 1/2$, i.e., for the small subregion A or in the near-flat limit. Together with the relation between anti-flatness and non local magic, Theorem 1, we find

$$M_{dist}^{(NL)}(\psi_{AB}) \ge \frac{1}{8} \left(\frac{\operatorname{Pur}(\psi_{A})}{4G} \right)^{2} \left| \frac{\partial \mathcal{A}}{\partial \mathcal{T}} \right|_{\mathcal{T}=0} \ge \frac{1}{8} \left(\frac{e^{-\mathcal{A}/4G}}{4G} \right)^{2} \left| \frac{\partial \mathcal{A}}{\partial \mathcal{T}} \right|_{\mathcal{T}=0} \propto \frac{1}{8} \left| \frac{\partial e^{-2\mathcal{A}/4G}}{\partial \mathcal{T}} \right|_{\mathcal{T}=0} (2.7)$$

the left-hand side is the magic in the CFT side, the right end side of the above equation is a measure of the back-reaction in AdS. As we prove in Section 5.1, the above equation also implies that back-reaction is non-zero only if non-local magic is non vanishing.

Further exploiting the structure of entanglement in CFT, (see Eq. (4.6),) we can also obtain a simpler relation that holds more generally without the $S_2(A) - S_3(\psi_A) < 1/2$ constraint.

$$\left| \frac{\partial \mathcal{A}}{\partial \mathcal{T}} \right|_{\mathcal{T}=0} \approx \frac{(4G)^2}{\kappa} \mathcal{M}_2^{NL}(\psi_{AB}) \tag{2.8}$$

which shows a more direct relation between gravitational back-reaction and non-local magic based on the stabilizer 2-Rényi entropy for some constant κ .

Now for more general CFTs that need not have holographic duals, the above relations continue to hold with suitable substitutions of $\mathcal{T} \to (n-1)/4Gn$ and $\mathcal{A}/4G \to \tilde{S}_n$ where \tilde{S}_n is a function of Rényi entropy defined by [75]. We present compelling evidence that an additive anti-flatness measure is proportional to the amount of non-local magic in the system. We show with analytical arguments and numerical results that the exact non-local magic in the CFT scales as S(A) whereas the smoothed non-local magic scales as $\sqrt{S(A)}$. We then conjecture that such relations hold for general CFTs and apply this conjecture to evaluate magic for selected examples in holographic CFT using Eq. (2.4). Specifically, we do so for the static thermofield double state, and for non-equilibrium dynamics after local and global quantum quenches. We also examine the magic evolution in a time-evolved wormhole geometry described by a thermal field double state.

3 Non-local Magic

3.1 Magic measures

In this section, we introduce several measures of magic that will be central to supporting the claims in this manuscript. In order to properly establish a magic state resource theory, it is essential that we define an initial null set for such a resource theory. To achieve this purpose, we introduce three null sets, which we label as PSTAB, STAB₀, and STAB. Then we derive the free operations on such sets.

Additionally, we must introduce several useful concepts: the Pauli group, the Clifford group, and the set of stabilizer quantum states. Consider the Hilbert space of single qudit $\mathcal{H} = \mathbb{C}^d$, on which we define the following Pauli operators

$$X|i\rangle = |i+1\rangle \quad Z|j\rangle = \omega^j|j\rangle,$$
 (3.1)

where $\omega \equiv \exp(2i\pi/d)$. The selection of operators in Eq. (3.1) likewise defines the qudit computational basis $\{|i\rangle\}_i^d$.

The Pauli group $\tilde{\mathcal{P}}$ is defined as follows

$$\tilde{\mathcal{P}} \equiv \langle \tilde{\omega} \mathbb{1}, X, Z \rangle \tag{3.2}$$

where $\langle \cdot \rangle$ labels the set generated by $\{\tilde{\omega} \mathbb{1}, X, Z\}$, and $\tilde{\omega} = \omega$ for d odd, and $\tilde{\omega} = \exp[i\pi/d]$ for d even. When the number of qudits is n, the Pauli group $\tilde{\mathcal{P}}_n$ is defined as the n-fold tensor product of the single qudit Pauli group $\tilde{\mathcal{P}}$.

The Clifford group $C(d^n)$ is defined as the normalizer of the Pauli group, meaning that for any $U \in C(d^n)$ we have $U^{\dagger} \tilde{\mathcal{P}}_n U \equiv \tilde{\mathcal{P}}_n$. The group $C(d^n)$ is a multiplicative matrix group. For qubits, d=2 it can be generated by the Hadamard, phase, and Controlled-Z quantum gates

$$H \equiv \frac{1}{\sqrt{2}} \begin{bmatrix} 1 & 1 \\ 1 & -1 \end{bmatrix}, \quad P \equiv \begin{bmatrix} 1 & 0 \\ 0 & i \end{bmatrix}, \quad CZ \equiv \begin{bmatrix} 1 & 0 & 0 & 0 \\ 0 & 1 & 0 & 0 \\ 0 & 0 & 1 & 0 \\ 0 & 0 & 0 & -1 \end{bmatrix}.$$
 (3.3)

For general d the generators are [81] the controlled-Z CZ, the quantum Fourier Transform F and the phase gate P, whose action of the d-computational basis is

$$CZ |ii'\rangle := \omega^{ii'} |ii'\rangle \quad F |i\rangle := \frac{1}{\sqrt{d}} \sum_{i \in \mathbb{Z}_d} \omega^{ii'} |i'\rangle \quad P |i\rangle := \omega^{s(s+\phi_d)/2} |s\rangle$$
 (3.4)

where $\phi_d = 1$ if d is odd, 0 otherwise. Notably, circuits composed of the Clifford gates in Eq. (3.3) can be efficiently simulated on a classical computer [66, 82].

At this point, one can define the notion of stabilizer states for pure states. We first say that a pure state $|\phi\rangle$ is stabilized by $P \in \tilde{\mathcal{P}}_n$ if $P|\phi\rangle = |\phi\rangle$. Then we define the pure stabilizer states as the set

$$PSTAB^{(n)} := \{ |\phi\rangle\langle\phi| = \frac{1}{|G|} \sum_{P \in G} P|G \subset \tilde{\mathcal{P}}_n, \ G \text{ abelian} \}$$
 (3.5)

with the cardinality of G is $|G| = d^n$ and G is a group of commuting Pauli operators. Notice that $PSTAB^{(n)}$ is the orbit through the Clifford group of any computational basis state for n qudits, i.e., $PSTAB^{(n)} = \{C|i_1 \dots i_n\rangle | C \in \mathcal{C}(d^n)\}$. The notion of pure stabilizer states conveys the fact of a set of resources that is closed under Clifford operations.

For mixed states, the most primitive notion of stabilizer states is that of [42] STAB₀, defined as the set of states $\sigma = \frac{1}{d^n} \sum P \in G$, where G is a group of commuting Pauli operators (see [83]). In [42], STAB₀⁽ⁿ⁾ is introduced as the set of states for which the stabilizer entropy (SE) is zero and SE is a good monotone for PSTAB⁽ⁿ⁾. From a more foundational perspective, STAB₀⁽ⁿ⁾ is the set of states that can be purified in PSTAB⁽ⁿ⁾ and they can only yield trivial probability distributions, see[76]

When one allows for general probabilities distributions we obtain the convex hull of $PSTAB^{(n)}$, namely $STAB^{(n)} := \{\sigma | \sigma = \sum_i p_i | \phi_i \rangle \langle \phi_i |, | \phi_i \rangle \in PSTAB^{(n)} \}$. Note that $STAB_0^{(n)} \subset STAB^{(n)}$.

The next step in the definition of our measures of magic is to define the free operations of $STAB^{(n)}$ and $STAB_0^{(n)}$. For $STAB^{(n)}$ the free operations are given in [41], and we list them here for the sake of completeness:

- 1. Clifford unitaries. $\rho \to U \rho U^{\dagger}$ with $U \in \mathcal{C}(d^n)$.
- 2. Composition with stabilizer states, $\rho \to \rho \otimes \sigma$ with σ a stabilizer state.
- 3. Computational basis measurement on the first qudit, $\rho \to (|i\rangle\langle i| \otimes \mathbb{1}_{n-1})\rho(|i\rangle\langle i| \otimes \mathbb{1}_{n-1})/\mathrm{Tr}(\rho|i\rangle\langle i| \otimes \mathbb{1}_{n-1})$ with probability $\mathrm{Tr}(\rho|i\rangle\langle i| \otimes \mathbb{1}_{n-1})$
- 4. Partial trace of the first qudit, $\rho \to \text{Tr}_1(\rho)$
- 5. The above operations conditioned on the outcomes of measurements or classical randomness.

It is straightforward to show that operations 1.-4. also apply to $STAB_0^{(n)}$ (see Appendix A). However, it's important to note that stabilizer operations conditioned on measurements or classical randomness do not belong to the set of free operations for $STAB_0^{(n)}$. This is an important feature of the $STAB_0^{(n)}$ resource theory as it counts non-flat probabilities as resources. It is the key element to use deviation from flatness as the resource that connects magic in CFT to geometry in AdS.

Given the notion of null sets and free operations, one can then proceed to introduce suitable measures of magic. Let us start by defining the trace distance of magic:

Definition 1 (Trace distance of magic₀). The trace distance of magic₀ of a state ψ is given by:

$$M_{dist}(\psi) := \min_{\sigma \in \text{STAB}_{0}^{(n)}} \frac{1}{2} \|\psi - \sigma\|_{1}$$
(3.6)

Proposition 1. The trace distance of magic satisfies the following properties:

- 1. Faithfulness: $M_{dist}(\rho) = 0$ if and only if ρ is a stabilizer state.
- 2. Monotonicity: for all completely positive trace-preserving channels ξ preserving STAB₀⁽ⁿ⁾, $M_{dist}(\xi(\rho)) \leq M_{dist}(\rho)$
- 3. Subadditivity: $M_{dist}(\rho_1 \otimes \rho_2) \leq M_{dist}(\rho_1) + M_{dist}(\rho_2)$

- *Proof.* 1. By definition $M_{dist}(\psi) = 0$ if and only $\psi \in STAB_0^{(n)}$, and so ψ is a stabilizer state.
 - 2. The monotonicity descends from the monotonicity of the trace distance under tracepreserving CP maps. Because given a map $\xi : STAB_0^{(n)} \mapsto STAB_0^{(n')}$ we have

$$M_{\text{dist}}(\xi(\rho)) = \min_{\sigma \in \text{STAB}_0^{(n')}} \frac{1}{2} \| \xi(\rho) - \sigma \|_1$$
 (3.7)

$$= \min_{\sigma \in \text{STAB}_0^{(n')}} \frac{1}{2} \| \xi(\rho - \sigma) \|_1$$
 (3.8)

$$\leq \min_{\sigma \in \xi(\text{STAB}_0^{(n)})} \frac{1}{2} \|\xi(\rho - \sigma)\|_1 \tag{3.9}$$

$$\leq \min_{\sigma \in \text{STAB}_0^{(n)}} \frac{1}{2} \|\rho - \sigma\|_1 = M_{\text{dist}}(\rho) \tag{3.10}$$

where we used that $STAB_0^{(n')} \subseteq \xi(STAB_0^{(n)})$, the proof of the last statement is straightforward. One must observe that since ξ is expressed in terms of stabilizer operations, the only operations that reduce the dimension are partial traces. Therefore, it is evident that since states in $STAB_0^{(n)}$ are mapped to stabilizer states in $STAB_0^{(n')}$ after a partial trace, the statement must hold true because there are more states whose partial trace returns the same state.

3. Subadditivity:

$$M_{\text{dist}}(\rho_L) = M_{\text{dist}}(\rho_1 \otimes \rho_2) = \frac{1}{2} \min_{\sigma \in \text{STAB}_0^{(n)}} \|\rho_1 \otimes \rho_2 - \sigma\|_1$$

$$= \frac{1}{2} \min_{\sigma \in \text{STAB}_0^{(n)}} \|\rho_1 \otimes \rho_2 - \sigma_1 \otimes \sigma_2 + \sigma_1 \otimes \sigma_2 - \sigma\|_1$$

$$\leq \frac{1}{2} \|\rho_1 \otimes \rho_2 - \sigma_1 \otimes \sigma_2\|_1 + \frac{1}{2} \min_{\sigma \in \text{STAB}_0^{(n)}} \|\sigma_1 \otimes \sigma_2 - \sigma\|_1$$

$$(3.12)$$

$$(3.13)$$

$$\leq \frac{1}{2} \| \rho_1 \otimes \rho_2 + \rho_1 \otimes \sigma_2 - \rho_1 \otimes \sigma_2 - \sigma_1 \otimes \sigma_2 \|_1 \qquad (3.14)$$

$$\leq \frac{1}{2} \|\rho_1\|_1 \|\rho_2 - \sigma_2\|_1 + \frac{1}{2} \|\sigma_2\|_1 \|\rho_1 - \sigma_1\|_1 \tag{3.15}$$

$$\leq \frac{1}{2} \|\rho_2 - \sigma_2\|_1 + \frac{1}{2} \|\rho_1 - \sigma_1\|_1 \tag{3.16}$$

where we used that σ_1, σ_2 are two stabilizer states, then $\min_{\sigma \in STAB_0^{(n)}} \|\sigma_1 \otimes \sigma_2 - \sigma\| = 0$, and the tightest bound is obtained by minimizing over σ_1 and σ_2 proving the statement.

One can also define an entropic quantity the Relative stabilizer entropy of magic:

Definition 2 (Relative Stabilizer Entropy of Magic). The relative stabilizer entropy of magic of ρ is given by

$$M_{RS}(\rho) = \min_{\sigma \in STAB_0^{(n)}} S(\rho||\sigma)$$
(3.17)

Proposition 2. The relative stabilizer entropy is a magic monotone, i.e., 1. it is zero iff $\rho \in STAB_0^{(n)}$, 2. is invariant under Clifford conjugation, 3. is non-increasing on average under stabilizer measurement, 4. is non-increasing under partial trace and 5. is invariant under stabilizer composition.

Proof. The proof is similar to [41, Appendix A], where the only difference is the definition of $STAB^{(n)}$. Here we recount for completeness.

- 1. Note that $S(\rho||\sigma) \ge 0$ where equality is attained iff $\rho = \sigma$. Hence it only vanishes when $\rho \in STAB_0^{(n)}$, which by our definition is a stabilizer state.
- 2. Recall that STAB₀ is invariant under Cliffords, therefore for $U \in \mathcal{C}(d^n)$

$$M_{RS}(U\rho U^{\dagger}) = \min_{\sigma \in \text{STAB}_0^{(n)}} S(U\rho U^{\dagger}||\sigma) = \min_{\sigma \in \text{STAB}_0^{(n)}} S(\rho||U^{\dagger}\sigma U) = \min_{\sigma \in \text{STAB}_0^{(n)}} S(\rho||\sigma).$$

3. The action of partial stabilizer measurements of the form $V_i = I \otimes |i\rangle\langle i|$ for some Pauli basis state $|i\rangle$ on STAB₀ returns a stabilizer state up to normalization. Using that $p_i = \text{Tr}[\rho V_i], q_i = \text{Tr}[\sigma V_i]$ and $\rho_i = V_i \rho V_i^{\dagger}, \sigma_i = V_i \sigma V_i^{\dagger}$, we can reuse the proof from [41] and note that

$$\sum_{i} p_{i} S\left(\frac{\rho_{i}}{p_{i}} \middle\| \frac{\sigma_{i}}{q_{i}}\right) \leq S(\rho||\sigma).$$

The rest follows because σ_i/q_i is again a stabilizer state.

- 4. By Lieb and Ruskai [84], it is shown that quantum relative entropy is non-increasing under partial trace, i.e., $S(\operatorname{Tr}_B(\rho_{AB})||\operatorname{Tr}_B(\sigma_{AB})) \leq S(\rho||\sigma)$.
- 5. It is known that for any state τ , $S(\rho \otimes \tau | | \sigma \otimes \tau) = S(\rho | | \sigma)$, hence the desired result follows when we take $\tau \in STAB_0^{(n)}$.

3.2 (Anti-)Flatness

Flatness is the property of a quantum state that describes how close its spectrum is to a flat spectrum. From the operational point of view, the flatness of a state describes how flat is the classical probability distribution over a basis of pure states in which we can decompose it. Of course, this does not imply that this state will return a flat probability distribution for the measurements in any other basis. As an example of flat states, both the completely mixed state and pure states possess flat spectrum. Another notable example [85] are the ground states of string-net Hamiltonians, e.g. the toric code and its generalizations.

Flat states are the free states for the resource theory of flatness. We thus define the null set as

$$FLAT^{(n)} := \left\{ \sigma \in \mathcal{H} \,|\, \sigma^2 = \frac{\sigma}{\operatorname{rank} \sigma} \right\}$$
 (3.18)

Let us now define the following measure of anti-flatness, that is, how far is a spectrum from the flat one. Of course, this quantity must measure the resource defined by $FLAT^{(n)}$.

Definition 3. We define the anti-flatness of ψ_A as [74]

$$\mathcal{F}(\psi_A) = \text{Tr}(\psi_A^3) - \text{Tr}^2(\psi_A^2) \tag{3.19}$$

This quantity is very natural as it can be defined classically as the variance of a probability distribution p(x) according to the probability distribution itself. More concretely, if one defines $\langle x \rangle_p := \sum_x xp(x)$, and one defines $\Delta p^2 := \langle (p - \langle p \rangle_p)^2 \rangle_p$, then one has

$$\mathcal{F}(\psi_A) = \Delta \lambda^2 \tag{3.20}$$

with $\{\lambda\} \equiv spec[\psi_A]$. Of course, this quantity is zero on the flat states, that is, $\mathcal{F}(\sigma) = 0$ for $\sigma \in FLAT^{(n)}$ as it is immediate to verify.

There is a profound connection between anti-flatness and magic. It connects magic, which is a property of the full state, to bipartite entanglement, and thus to the spectrum of a reduced density operator. In particular, it has been shown that [74], given a pure state ψ_{AB} in a bipartite Hilbert space $\mathcal{H} = \mathcal{H}_A \otimes \mathcal{H}_B$, its linearized stabilizer entropy M_{lin} is the average anti-flatness of ψ_A on the Clifford orbit, that is,

$$\langle \mathcal{F}(\psi_A^C) \rangle_C = f(d_A, d_B) M_{lin}(\psi_{AB})$$
 (3.21)

where $\psi_A^C = \text{Tr}_B \psi_{AB}^C \equiv \text{Tr}_B(C\psi_{AB}C^{\dagger})$. It is also true that anti-flatness shows typicality. Later, we will use this property to connect magic to spectral properties. The main message of Eq. (3.21) is that, as long as the state ψ is very entangled, and therefore ψ_A is full rank, one can use the spectral quantity $\mathcal{F}(\psi_A)$ to probe magic. Note that - by definition - every density matrix is full rank on its support. This will come in handy in the next section.

It is possible to define another monotone for the resource theory of flatness through the quantum relative entropy,

$$\mathcal{F}_R(\rho) = \min_{\sigma \in \text{FLAT}^{(n)}} S(\rho \| \sigma). \tag{3.22}$$

One can prove the following proposition

Proposition 3. Given a state $\rho \in \mathcal{H}$, it holds that

$$\mathcal{F}_R(\rho) = S_{max}(\rho) - S(\rho) \tag{3.23}$$

See Appendix A.1 for a proof. Note that $\mathrm{FLAT}^{(n)} \supset \mathrm{STAB}_0^{(n)}$ where $\mathrm{STAB}_0^{(n)}$ is the set of states with zero stabilizer Rényi entropy, hence $\min_{\sigma \in \mathrm{STAB}_0^{(n)}} S(\rho||\sigma) \geq F_R(\rho)$, therefore the flatness lower bounds the total subregion magic for any state. The same would not be

true if $STAB^{(n)}$ is the usual stabilizer polytope, because it overlaps with $FLAT^{(n)}$ but is not a subset as one can take a classical mixture of it such that the eigenvalues of ρ are not equal (or zero).

Finally, let us define yet another flatness that will be natural for holography. Recall from [86] that a variant of the Rényi entropy is given by,

$$\tilde{S}_n(\rho) = n^2 \partial_n \left(\frac{n-1}{n} S_n(\rho) \right) = -n^2 \partial_n \left(\frac{\log \operatorname{Tr}(\rho^n)}{n} \right). \tag{3.24}$$

If we rewrite $Tr(\rho^n)$ in terms of the spectrum $\{\lambda_k\}$ of ρ , it becomes

$$\tilde{S}_n(\rho) = -n^2 \partial_n \left(\frac{\log(\sum_k \lambda_k^n)}{n} \right) = \log(\sum_k \lambda_k^n) - n \frac{\sum_k \lambda_k^n \log \lambda_k}{\sum_k \lambda_k^n}.$$
(3.25)

Now we take the derivative of this expression and obtain another definition of antiflatness. In fact, this quantity is known as the *Capacity of Entanglement*, which has been explored in the context of condensed matter system [87, 88] and in quantum gravity [89–92].

Proposition 4. $\partial_n \tilde{S}_n(\rho)$ is a measure of anti-flatness in that $\partial_n \tilde{S}_n(\rho) = 0$ if and only if ρ has a flat spectrum.

Proof. Expanding the definition using the set of eigenvalues of ρ .

$$\partial_n \tilde{S}_n(\rho) = -n \frac{(\sum_k \lambda_k^n \log^2 \lambda_k)(\sum_l \lambda_l^n) - (\sum_k \lambda_k^n \log \lambda_k)^2}{(\sum_k \lambda_k^n)^2}$$
(3.26)

$$= -n \frac{(\sum_{kl} \lambda_k^n \lambda_l^n \log^2 \lambda_k) - (\sum_{kl} \lambda_k^n \lambda_l^n \log \lambda_k \log \lambda_l)}{(\sum_k \lambda_k^n)^2}$$
(3.27)

$$= -n \frac{\sum_{(kl)} \lambda_k^n \lambda_l^n (\log^2 \lambda_k + \log^2 \lambda_l - 2\log \lambda_k \log \lambda_l)}{(\sum_k \lambda_k^n)^2}$$
(3.28)

$$= -n \frac{\sum_{(kl)} \lambda_k^n \lambda_l^n \log^2 \frac{\lambda_k}{\lambda_l}}{(\sum_k \lambda_k^n)^2}, \tag{3.29}$$

where $\sum_{(kl)}$ denotes sum over each pair of distinct indices $k \neq l$. Note that each term in the numerator is non-negative. Therefore $\partial_n \tilde{S}_n = 0$ if and only if $\log \frac{\lambda_k}{\lambda_l} = 0$, which is equivalent to $\lambda_k = \lambda_i$ for all k, l.

This anti-flatness (Eq. (3.26)) can be connected to (Eq. (3.19)) by first noticing that the anti-flatness $\mathcal{F}(\rho)$ corresponds to the variance of ρ . The proof is straightforward

$$\mathcal{F}(\rho) = \operatorname{tr}(\rho^3) - \operatorname{tr}^2(\rho^2) = \operatorname{tr}(\rho \rho^2) - \operatorname{tr}^2(\rho \rho) = \langle \rho^2 \rangle_{\rho} - \langle \rho \rangle_{\rho}^2 = \operatorname{Var}_{\rho}(\rho)$$
 (3.30)

Let us connect this definition with the derivative at n=1. Let $\rho \equiv \sum_k \lambda_k |\lambda_k\rangle \langle \lambda_k|$. Note that the following relation can also be written as a variance, by defining $p_k = \frac{\lambda_k^n}{\sum_k \lambda_k^n}$, it is easy to observe that $\sum p_k = 1$ and we can define the state

$$\Xi := \sum_{k} p_k |\lambda_k\rangle\langle\lambda_k| \tag{3.31}$$

and so

$$\partial_n \tilde{S}_n(\rho) = -n \sum_{kl} p_k p_l(\log^2 \lambda_k - \log \lambda_k \log \lambda_l)$$
(3.32)

$$= -n\langle \log^2 \rho \rangle_{\Xi} + n\langle \log \rho \rangle_{\Xi}^2 = -n \operatorname{Var}_{\Xi}(\log \rho)$$
 (3.33)

Let us compute it for n=1

$$\partial_n \tilde{S}_n(\rho)\Big|_{n=1} = -\sum_{kl} \lambda_k \lambda_l \log \lambda_k (\log \frac{\lambda_k}{\lambda_l})$$
 (3.34)

$$= -\sum_{k} \lambda_{k} \log^{2} \lambda_{k} + \sum_{kl} \lambda_{k} \lambda_{l} \log \lambda_{k} \log \lambda_{l}$$
(3.35)

$$= -\operatorname{tr}(\rho \log^2 \rho) + \operatorname{tr}^2(\rho \log \rho) \tag{3.36}$$

$$= -\langle \log^2 \rho \rangle_{\rho} + \langle \log \rho \rangle_{\rho}^2 = -\operatorname{Var}_{\rho}(\log \rho) \tag{3.37}$$

Interestingly, when n = 1, Ξ coincides with ρ . Seeing $\log \rho$ as a function of ρ , the variances between the two quantities are connected. We make use of standard techniques of error propagation to get the relationship between $\operatorname{Var}_{\rho}(\rho)$ and $\operatorname{Var}_{\rho}(\log(\rho))$.

$$\operatorname{Var}_{\rho}(\log(\rho)) \approx \frac{\operatorname{Var}_{\rho}(\rho)}{\langle \rho \rangle_{\rho}^{2}} = \frac{\operatorname{Var}_{\rho}(\rho)}{\operatorname{Pur}(\rho)^{2}} = \frac{\mathcal{F}(\rho)}{\operatorname{Pur}^{2}(\rho)}, \tag{3.38}$$

The approximation is valid when $S_0(\rho) - S_2(\rho) < \log 2$. Therefore, the two measures coincide in the near-flat or weak entanglement regime.

In fact, Eq. (3.26) has a convenient rewriting as the variance of the modular Hamiltonian. Given a state $\rho \equiv \sum_k \lambda_k |\lambda_k\rangle\langle\lambda_k|$, its eigenvalues can be written as $\lambda_k := \exp(-\beta E_k)$ where β is an effective temperature. Note that since $\sum_k \lambda_k = 1$ then $Z[\beta] = 1$. This also defines the (entanglement) Hamiltonian

$$H = \sum_{k} E_k |\lambda_k\rangle\langle\lambda_k| \tag{3.39}$$

From (Section 3.2), we get

$$\left. \partial_n \tilde{S}_n(\rho) \right|_{n=1} = -\sum_k \exp(-\beta E_k) (-\beta E_k)^2 + \left(\sum_k \exp(-\beta E_k) (-\beta E_k) \right)^2$$

$$= -\beta^2 \left[\langle H^2 \rangle_\beta - \langle H \rangle_\beta^2 \right]$$
(3.40)

also, with simple algebra, one obtains that

$$\partial_n \tilde{S}_n(\rho) \Big|_{n=1} = -\beta^2 \left[\langle H^2 \rangle_\beta - \langle H \rangle_\beta^2 \right] = -\beta^2 \langle (E_k - E_l)^2 \rangle_{kl}$$
 (3.42)

In other words, the modified Rényi entropy is proportional - by inverse temperature - to the fluctuations of the Hamiltonian H which in turn is the average gap squared in the energies E_k . This also shows why the derivative is connected to the anti-flatness of the state.

This result can be extended to any n, to do this, note first that $\Xi = \exp(-n\beta H)Z^{-1}[n\beta]$. Then with some algebra, we obtain

$$\partial_n \tilde{S}_n(\rho) = -n^3 \beta^2 (\langle H^2 \rangle_{n\beta} - \langle H \rangle_{n\beta}^2). \tag{3.43}$$

3.3 Non-local Magic, Entropy, and anti-Flatness

In this section, we are going to introduce the concept of *non-local magic*, and how it relates to both entanglement and anti-flatness.

Definition 4 (Multi-partite non-local magic). Given M a measure of magic and $\psi_{A_1...A_n} \equiv |\psi_{A_1...A_n}\rangle\langle\psi_{A_1...A_n}|$ a pure state, we define as n-partite non-local magic

$$M^{(n-NL)}(\psi_{A_1...A_n}) := \min_{U = \bigotimes_{i=1}^n U_{A_i}} M(U\psi_{A_1...A_n} U^{\dagger}). \tag{3.44}$$

As we exclusively discuss the case of bipartite non-local magic when n=2 for the rest of this work, we set $A=A_1, B=A_2$ and simply refer to $M^{(NL)}=M^{(2-NL)}$ as non-local magic for convenience.

Intuitively, non-local magic is the non-stabilizerness that lives in the correlation between A and B because $U_A \otimes U_B$ removes all "local" magic in A or B separately. This is distinct from other notions of long-range magic [44, 93, 94]. Note that A, B themselves can be multi-qubit systems, so U_A, U_B need not be single qubit unitaries.

In this work, we will use as measures of magic $M_{\rm dist}$ and the two relative entropies of magic M_R , M_{SR} .

3.3.1 Non-local magic and flatness

Let us start with a general relation valid for *any* measure of anti-flatness and *any* measure of non-local magic.

Lemma 1. A pure quantum state $|\psi\rangle$ possesses no non-local magic, that is, $M^{NL}(|\psi\rangle) = 0$, iff $|\psi\rangle$ is unitarily locally equivalent to a state $|\psi'\rangle = U_A \otimes U_B |\psi\rangle$ with flat reduced density matrix $\psi'_A \equiv \operatorname{tr}_B |\psi'\rangle\langle\psi'|$ with integer Rényi entropies². In formulae,

$$M_{NL}(|\psi\rangle) = 0 \iff F(\psi_A) = 0 \land \operatorname{rank}(\psi_A) = d^{r_A}, \ r_A \in \mathbb{N}$$
 (3.45)

Proof. Let us start from the left-to-right implication. We employ the fact that any faithful measure of magic $M(|\psi\rangle)$ vanishes on the free states. For any such measure, its non-local counterpart with respect to the bipartition A|B is $M^{NL}(|\psi\rangle) := \min_{U_A \otimes U_B} M(U_A \otimes U_B|\psi\rangle)$. Given $M^{(NL)}(|\psi\rangle) = 0$, then we know that there exist a bi-local unitary $U_A \otimes U_B$ such that $|\psi'\rangle \equiv U_A \otimes U_B|\psi\rangle \in \text{STAB}_0^{(n)}$. Since $\text{STAB}_0^{(n)}$ is closed under partial trace, see Section 3.1, then $\psi'_A \in \text{STAB}_0^{(n)}$. We know that $\psi'_A \in \text{FLAT}^{(n)}$. Moreover, being $\psi'_A \in \text{STAB}_0^{(n)}$ we know that $\text{rank}(\psi_A) = d^{r_A}$ with $r_A \in \mathbb{N}$. Let us now show that also the converse is true. Consider a flat state $|\psi\rangle$, that is, a state such that its reduced density matrix $\psi_A \equiv \text{tr}_B |\psi\rangle\langle\psi| = \frac{1}{d^{r_A}} \sum_i |\phi_i\rangle\langle\phi_i|_A$ where the sum run on d^{r_A} many rank-one projectors $|\phi_i\rangle\langle\phi_i|_A$. Note that we exploited the fact that $S_\alpha(A) = r_A \in \mathbb{N}$ for every $\alpha \in [0, \infty)$. Via the Schmidt decomposition, we can write the state as $|\psi\rangle = \sum_i \frac{1}{\sqrt{d^{r_A}}} |\phi_i\rangle_A \otimes |\psi_i\rangle_B$. Without loss of generality, we choose now |A| < |B|. We further know that $\langle\phi_i|\phi_i\rangle = \langle\psi_i|\psi_i\rangle = \delta_{ij}$.

 $^{^2}$ In this work, information is measured using bits. Accordingly, entropies are computed using \log_d .

Now choose U_A (resp. U_B) such that $U_A|\phi_i\rangle_A = |i\rangle_A$ (resp. $U_B|\psi_i\rangle_B = |i\rangle_B$) for $|i\rangle_A$ (resp. $|i\rangle_B$) being the computational basis on A (resp. B). We obtain

$$U_A \otimes U_B |\psi\rangle = \sum_i \frac{1}{\sqrt{d^{r_A}}} |i\rangle_A \otimes |i\rangle_B \equiv |EPR\rangle_{A\bar{A}} \otimes |j\rangle_{B\backslash\bar{A}}$$
(3.46)

where $|EPR\rangle_{A\bar{A}}$ is a EPR pair between the full A and any subsystem $\bar{A} \subset B$ such that $|A| = |\bar{A}|$, while $|j\rangle$ is a computational basis state on $B \setminus \bar{A}$. Since $|EPR\rangle_{A\bar{A}} \otimes |j\rangle_{B\setminus\bar{A}}$ is a stabilizer state, we obtain

$$0 = M(U_A \otimes U_B | \psi \rangle) \ge \min_{U_A \otimes U_B} M(U_A \otimes U_B | \psi \rangle) = M^{NL}(|\psi \rangle) \ge 0$$
 (3.47)

Notice that a vanishing non-local magic is a sufficient condition for anti-flatness to be zero. However, there are possibly states with non-integer Rényi entropies that can possess some non-local magic without being guaranteed that anti-flatness is non-vanishing. With the additional condition of integer Rényi entropy, also the other implication holds, that is, a flat state implies vanishing non local magic for any sensible measure of non local magic.

We now show lower and upper bounds to the non-local magic based on the trace distance of M_{dist} defined in Definition 1. As we saw previously, anti-flatness connects magic and entanglement. We have:

Theorem 1. Let ψ_{AB} be a pure state in a bipartite Hilbert space $\mathcal{H} = \mathcal{H}_A \otimes \mathcal{H}_B$, then

$$\mathcal{F}(\psi_A)/8 \le M_{dist}^{(NL)}(\psi_{AB}) \le \sqrt{1 - e^{S_{max}(A)} + e^{S_{\infty}(A)} \left(1 - \frac{e^{\log(d) \lfloor S_{max}(A)/\log d \rfloor}}{e^{S_{max}(A)}}\right)}$$
(3.48)

where $\lfloor \cdot \rfloor$, is the floor function. The proof can be found in the Appendix B.

As we shall see in Section 5.1, the Lemma 1 and Theorem 1 will have important consequences for the relationship between the non-local magic in the CFT side and gravity in AdS.

3.3.2 Non-local stabilizer relative entropies of magic

In this section, we show that similar to the trace distance of magic, the relative stabilizer entropy also has a tight connection with flatness and entanglement.

Theorem 2. Let ψ_{AB} be a pure state, then

$$S_{max}(A) - S(A) = \mathcal{F}_R(\psi_A) \le \min_{U_A} M_{RS}(U_A \psi_A U_A^{\dagger}) \le M_{RS}^{(NL)}(\psi_{AB}) \le \log d \lceil S_{max}(A) / \log d \rceil.$$
(3.49)

Here $S(A) = S(\rho_A)$ and $S_{max}(A) = S_{max}(\rho_A)$. The proof can be found in Appendix C.1. Let us briefly comment on the tightness of the bound. It is clear that when $|\psi\rangle_{AB}$ has a dominant Schmidt coefficient and many small trailing singular values, then the bound is essentially tight. A case in point is $\sqrt{1-\epsilon}|00\rangle + \sqrt{\epsilon}|11\rangle$. However, the upper

bound is quite loose for states with near-flat spectrum, e.g. $\epsilon = 1/2$. This is an artifact of choosing the maximally mixed state as a reference even though other stabilizer states clearly yield a lower distance.

A similar upper bound can be obtained with the usual relative entropy measure of magic.

Proposition 5 (Entanglement upper bounds NL magic). Suppose ρ_{AB} is pure, and

$$M_R^{(NL)}(\rho_{AB}) = \min_{U_A \otimes U_B} M_R((U_A \otimes U_B)\rho_{AB}(U_A \otimes U_B)^{\dagger}), \tag{3.50}$$

then $M_R^{(NL)}(\rho_{AB}) \leq S(A) = S(B)$, where S(A) is the von Neumann entropy of subsystem A.

The proof is given in Appendix C.2. This upper bound suffers from the same drawbacks as (Eq. (3.49)) for states that are maximally entangled.

3.3.3 Magic estimates

As minimization can be difficult for the relative entropy measure, let's also derive a tighter upper bound based on a computable measure of magic, that is, the stabilizer Rényi entropy. To do so, we can pick a good estimate that is reasonably close to the minimum. Suppose the entanglement spectrum of the state under the same bipartition AB is $\{\lambda_i\}$, construct a state

$$|\psi'\rangle_{AB} = \sum_{i=0}^{2^n - 1} \sqrt{\lambda_i} |s_i\rangle |s_i\rangle, \tag{3.51}$$

where $\{|s_i\rangle\}$ are eigenstates of a stabilizer group $\mathcal{S} = \{S_1, S_2, \dots, S_n\}$ such that for any S_k in \mathcal{S} , $S_k|s_i\rangle = \pm |s_i\rangle$. Because the entanglement spectrum is invariant under local unitary $U_A \otimes U_B$, $|\psi'\rangle$ is a reasonable construction such that the reduced density matrix on both A and B are within the *stabilizer polytope*, and hence have vanishing local magic by the relative entropy measure M_R . Note that other choices of the Schmidt basis may yield lower overall magic on AB, therefore $M(|\psi'\rangle)$ provides an upper bound of non-local magic.

We now present an estimate of $M(|\psi'\rangle)$ using the Stabilizer Rényi Entropy measure.

Proposition 6. The non-local stabilizer Rényi entropy estimate for a state with entanglement spectrum $\{\lambda_i\}$ is

$$\mathcal{M}_2(\{\lambda_i\}) = \mathcal{M}_2(\sum_{i=0}^{2^n - 1} \sqrt{\lambda_i} |s_i\rangle |s_i\rangle), \qquad \lambda_i \ge \lambda_j, \quad \text{for } i < j.$$
 (3.52)

Note that this non-local magic estimate doesn't depend on the choice of stabilizer group S. However, the ordering of eigenvalues does affect its magnitude. Remarkably, one can obtain an exact expression for $\mathcal{M}_2(\{\lambda_i\})$. A similar expression has also been obtained by [95] but in a different context. With additional ancillae, it is identical to the one below after applying a global Clifford unitary.

Theorem 3. The non-local stabilizer Rényi entropy estimate is

$$\mathcal{M}_2(\{\lambda_i\}) = -\log \left(\sum_{i_1, i_2, i_3, i_4 = 0}^{2^n - 1} \sqrt{\lambda_{i_1} \lambda_{i_2} \lambda_{i_3} \lambda_{i_4} \lambda_{i_3 \wedge i_2 \wedge i_1} \lambda_{i_4 \wedge i_2 \wedge i_1} \lambda_{i_1 \wedge i_3 \wedge i_4} \lambda_{i_2 \wedge i_3 \wedge i_4}} \right), \quad (3.53)$$

where \land denotes the bitwise XOR operation. This expression depends on the ordering of the eigenvalues and reaches its minimum when the eigenvalues are in the descending order, that is, $\lambda_i \geq \lambda_j$ for i < j.

In Section 4.2 we present numerical results of $\mathcal{M}_2(\{\lambda_i\})$ for finite-sized physical system. It is helpful to see that the estimate constitutes a non-local magic upper bound.

Corollary 3.1. Let $\{\lambda_i\}$ be the Schmidt values for $|\psi\rangle_{AB}$ when bipartitioning the system into A and B. The non-local stabilizer Rényi entropy is upper bounded by

$$\mathcal{M}_{2}^{NL}(|\psi\rangle_{AB}) \le \mathcal{M}_{2}(\{\lambda_{i}\}) \le \min\{2S_{2}(A), 4(S_{max}(A) - S_{1/2}(A))\}$$
 (3.54)

where
$$S_{max}(A) = n \log 2$$
, $S_{\alpha}(A) = S_{\alpha}(\rho_A)$ with $\rho_A = \text{Tr}_B[|\psi\rangle\langle\psi|]$.

See Appendix D for the proof. Based on this result, we discuss two regimes. One is when the spectrum is almost flat. In this regime, the bipartite non-local magic is upper bounded by,

$$\mathcal{M}_2(\{\lambda_i\}) \le 4(S_{\max}(A) - S_{1/2}(A)).$$
 (3.55)

This has the interpretation as anti-flatness. Although the measure of magic is different, we see that this gives a much tighter bound compared to (Theorem 2) in the near-flat regime.

Remark 1. Haar random states have small bipartite non-local magic.

We see that $\mathcal{M}_2 \sim S_0 - S_{1/2}$ whereas the lower bound from relative stabilizer entropy measure in (Theorem 2) is $S_0 - S_1$, both are bounded by a constant for Haar random states[96] — for small α , dim $A \ll \dim B = m$, $S_0 - S_\alpha \leq \frac{\alpha}{2} + O(1/m^2)$. This is somewhat surprising because Haar random states are magic rich and have non-trivial total magic [97, 98]. However, the magic sustained by their bipartite entanglement is small even though local magic in any subregion A with $|A| \gg |B|$ can be large.

Another limit is when $S_0(A) \gg S_{1/2}(A)$, which applies for quantum field theory. In this regime the magic is approximated by the second Rényi entropy,

$$\mathcal{M}_2(\{\lambda_i\}) \le 2S_2(A). \tag{3.56}$$

As we shall see in Section 4, this is consistent with our MERA intuition for conformal field theories.

3.3.4 Smoothed magic

The concept of magic and its bound, as discussed earlier, are applicable to systems with finite dimensions. However, in quantum field theory, the Hilbert space has an infinite dimension. In this case, the bounds given by max entropy in Theorem 2 can easily be

divergent. To produce a non-trivial bound, it is imperative to introduce the 'smoothed magic', defined as

$$M_{RS}^{\epsilon}(\rho) := \min_{\|\chi - \rho\| < \epsilon} M_{RS}(\chi), \tag{3.57}$$

as well as the 'smoothed non-local magic', defined as

$$M_{RS}^{(NL,\epsilon)}(\rho_{AB}) := \min_{\|\chi_{AB} - \rho_{AB}\| < \epsilon} M_{RS}^{(NL)}(\chi_{AB}).$$
 (3.58)

For this, a smoothed version of Theorem 2 holds.

Theorem 4. Let ρ_{AB} be a pure state, then

$$S_{max}^{\epsilon}(\rho_A) - (1 - \epsilon)^{-1} S(\rho_A) \le M_{RS}^{(NL,\epsilon)}(\rho_{AB}) \le \log d \lceil S_{max}(A)^{\epsilon} / \log d \rceil. \tag{3.59}$$

where the smoothed maximal entropy is defined as

$$S_{max}^{\epsilon}(\rho) = \min_{\|\chi - \rho\| < \epsilon} \ln(\operatorname{rank}(\chi)). \tag{3.60}$$

The proof can be found in Appendix C.3. As stated by Theorem 4, the magic is bounded from below by the difference between the smoothed maximal entropy and the entanglement entropy which is finite for conformal field theories.

Before we discuss CFTs, let's examine the physical meaning of the lower bound, which is the difference between smoothed max entropy and the von Neumann entropy. In addition to the anti-flatness of the entanglement spectrum, this quantifies the *compressibility* of a state [99]. Consider a bipartition of the state followed by a Schmidt decomposition. It is compressible if we can still well approximate it after truncating the less significant singular values, as one is wont to do in DMRG. Here we can show that this compressibility gap which lower bounds smoothed non-local magic also quantifies the classical hardness in simulations.

Let us build up the following argument by recalling that there are states such as random stabilizer states that have high entanglement but are classically easy to simulate. Since magic and entanglement capture two orthogonal perspectives of quantumness, are there quantum states with low entanglement but high magic that are classically hard to simulate? Naïvely, a state with high magic will have high stabilizer rank, which is hard in the stabilizer simulation. On the other hand, the system will be classically hard using the tensor network method if it has high bond dimensions. However, a folk theorem in tensor network suggests that the small entanglement would permit one to capture the state with a tensor network whose bond dimension only needs scale as $O(e^S)$ where S is the von Neumann entropy of each subsystem. Therefore, it seems that as long as the entanglement is small, there should be a classically easy description. However, one needs to be careful in applying this lore as it is known that there exist states with low entanglement but classically complex[100].

More precisely, consider an exact MPS description of a state with low entanglement such that for any subsystem A, $S(A) \ll \log \operatorname{rank}(\rho_A)$ where we have taken the bond dimension χ to be sufficiently large to reproduce the state exactly. One would be tempted to truncate the singular values and only keep $O(e^S)$ as suggested by the folk theorem. However, we note that this truncation is only justified if there exists σ_A with $||\sigma_A - \rho_A|| < \epsilon$ such that

$$\Delta S_{\epsilon}(A) = S_{\max}^{\epsilon}(A) - S(A) = \log \operatorname{rank}(\sigma_A) - S(A)$$

is small compared to S(A). In other words, the state is (perfectly) compressible. Such is indeed true for conformal field theory ground states, where $\Delta S_{\epsilon} \sim \sqrt{S \log(1/\epsilon)}$. However, this is not true in general. For example, consider a state $|\psi\rangle = \frac{1}{N} \sum_{i=1}^{r} \frac{1}{\sqrt{i}} |i\rangle_A |i\rangle_B$. The smoothed max entropy $S_{max}^{\epsilon} = \log r - \epsilon$, while entanglement entropy is nearly half of it, $S \approx \frac{1}{2} \log r$. In holography, [99] argued that certain state mixtures, such as that of a thermal and pure state, can lead to an arbitrarily large $\Delta S_{\epsilon}(A)$.

Therefore, high incompressibility on the one hand forces high tensor network bond dimension, and on the other necessitates high non-local magic from Theorem 4. This implies that such states will be classically hard to simulate and sharpens a general empirical observation that relates magic to classical complexity. Furthermore, if $S \ll \Delta S_\epsilon \approx S_{\rm max}^\epsilon$, then both the lower and upper bounds are approximately saturated. In this case, the smoothed non-local magic provides a quantitative measure for the classical hardness of simulating such states. Treating magic as roughly as the log of stabilizer rank and bond dimension, one would expect that classical resource of order $O(\exp(M_{RS}^{(NL,\epsilon)}))$ will be needed. It then follows that simulating such incompressible states is classical hard using not only the tensor network method but also the stabilizer and the Monte Carlo method [73] by having large magic³.

4 Magic in conformal field theories

Having seen a quantitative connection between anti-flatness in entanglement spectrum and non-local magic, we examine these relations in the context of CFTs.

4.1 Geometric Interpretation through tensor networks

To figure out (1) how much non-local magic there is in a CFT and (2) how such magic connected with the anti-flatness of the entanglement spectrum, it is instructive to first look at an intuitive picture from tensor networks. For CFTs with small central charges, MERAs have been shown to be good approximations of CFT ground states $|\psi\rangle_{AB}$. By extension, it also holds for products of CFTs with small central charge. Let us assume that the tensor network structure remains valid for arbitrary degree of accuracy, perhaps at the cost of increasing the bond dimension, which is supported by empirical observations. Using this as a heuristic, we deduce that local unitary deformations $U_A \otimes U_B$ unitarily "distills" an entangled state⁴ between A and B with log Schmidt rank that is upper bounded by the number of edge cuts (green triangle Fig. 1). As such cuts scale linearly with the size of the RT surface, i.e. the boundary of the triangle in the bulk, the log of Schmidt rank must be bounded by the number of edge cuts which scale the same way as entanglement entropy in this case. This implies that the non-local Magic in CFTs should scale linearly with the area of the Ryu-Takayanagi surface.

³A careful treatment of this problem should include other formulations of non-magical processes like Gaussian states, matchgates with [43].

⁴For simplicity, we will refer to such a process as distillation from now on. However, one should note that it is distinct from the usual entanglement distillation of perfect Bell pairs unless otherwise specified.

In fact, we can almost identify the optimal distilled state that has the same Schmidt rank but removes the unnecessary zero eigenvalues by just acting mostly unitaries and disentanglers. Let the blue rectangles at the bottom layer be the CFT ground state but at a more coarse-grained scale. As the ground state is an IR fixed point, we can simply use it as an input in the MERA to generate the more fine-grained state on the top layer. We can decompose the IR state by Schmidt decomposition, and the Schmidt rank is upper bounded by the bond dimension (here the bond is represented as 3 edges on each side of the blue rectangle on the bottom assuming the worst case volume law upper bound in the central region). By acting disentanglers and isometries in B followed by global unitaries on the subsystems represented by the blue rectangles on two sides of the bottom layer in the the IR ground state, we "pushed" the subregion B on the top layer to the red boundary by acting U_B , which now lives on ∂B . Similarly, acting U_A by running unitaries and isometries in A, we remove the bulk dof and push A to ∂A , marked by the orange lines. The qubits on ∂A and ∂B are entangled and their entanglement spectrum is unchanged since we only applied unitaries $U_A \otimes U_B$.

Let $|\partial A|, |\partial B|$ be the number of edges in $\partial A, \partial B$. The distilled state $|\chi\rangle_{AB}$ is not optimal as $\log rank(\rho_A) \leq |\partial A| < |\partial B|$, where we would have hoped that $|\partial A| = |\partial B| = \log rank(\rho_A)$, but this is close enough as $|\partial A|$ and $|\partial B|$ both scale as $\sim \log |A|$ as the blue region that contributed to suboptimality in the edge cuts is only constant (AdS) radius away from the true minimal surface. The number of edge cuts on the bottom layer is always bounded as the width of the MERA past causal cone is bounded. This means that $|\partial A| + const = |\partial B|$ where the constant depends on the network discretization. For binary MERA it stabilizes at 4 to 6 sites.

As a consequence, after the removal of local magic in each wedge, the remaining magic is tied up into the interface between A and B marked by the region shaded in blue. Since the amount of magic generically scales linearly with the number of tensors, for a contiguous subregion A, the size of the interface region scales as $\log |A|$, which is proportional to the size of the RT surface up to subleading corrections. Note that while it may be possible to lower the size of this interface region further by local unitary transformations, the number of sites it involves must be lower bounded by the minimum number of edges connecting A and B, which is given by $|\partial A|$. Heuristically, consider a case where all the bipartite entanglement between A and B have been "distilled" into imperfect Bell pairs connecting the two complementary regions. Then for any additive measure of magic, the non-local magic should scale linearly with the number of such imperfect Bell states, which is again proportional to the length of the minimal surface.

More precisely, we observe that the tensor network of the interface region is a matrix product state (MPS) (Fig. 2b) by removing the local unitaries. The remaining structure contributes to the non-local magic is shown in Fig. 2a. Each matrix in the chain consists of two isometries and one disentangler.

$$|\chi\rangle_{AB} = M_1^{(s_1r_1)} M_2^{(s_2r_2)} \cdots M_n^{(s_nr_n)} |s_1s_2\cdots s_n\rangle_{\partial A} |r_1r_2\cdots r_n\rangle_{\partial B}. \tag{4.1}$$

We expect the magic of this state to scale linearly with the number of matrices, namely

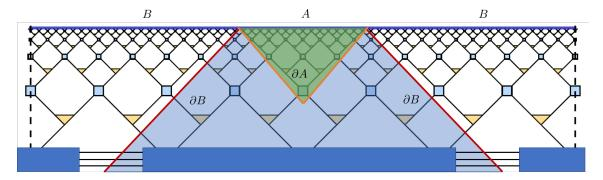


Figure 1: Green: past causal domain of dependence of A, Union of blue and green: past causal cone of A. Time runs upwards.

the size of the light-cone, $\min\{|\partial A|, |\partial B|\}$. Indeed, we verify that magic scales as volume of the MPS, which is $\sim \log |A|$.

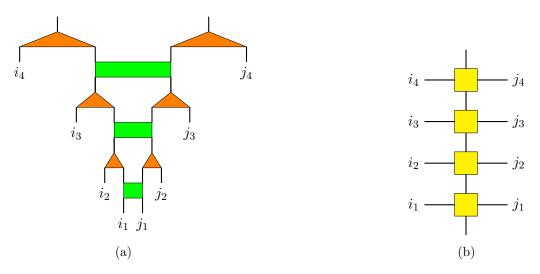
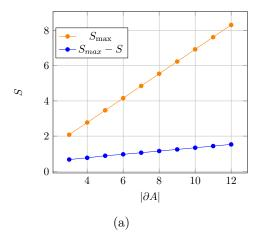


Figure 2: The MERA tensor network with local unitaries removed produces a tensor network (a) that contributes to non-local magic. It can be written as an MPS (b) for which its stabilizer Rényi entropy can be computed numerically.

For the numerics, we pick a random realization of the disentangler and isometry and use them for each each layer, in accordance of the scaling invariance. Then we present two estimations of the non-local magic of this MPS state. The first estimation we calculate the lower bound of the stabilizer relative entropy, given in Eq. (3.49). We present the result in Fig. 3a. Both max entropy and the von Neumann entropy scale linearly with the number of matrices, and thus linearly with respect to the RT surface area and the entanglement entropy S(A) of the boundary theory of subregion A. In the second estimation we calculate the entanglement spectrum of this state, denoting the set of eigenvalues as $\{\lambda_i\}$. Then we construct a state with the same entanglement spectrum and compute its non-local magic estimate using 3.52.



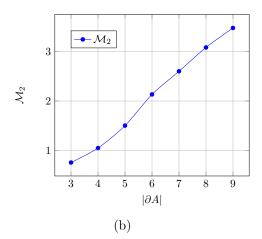


Figure 3: (a) Maximal entropy and von Neumann entropy of the MPS as a function of the number of sites in the state. (b) Stabilizer Rényi entropy of the state with small local magic.

The above intuition is also apparent when we think of the holographic QECC perspective of AdS/CFT where it is given by a code that corrects erasures approximately. In this case, complementary [22] approximate erasure correction promises the existence of recover unitaries supported on each subregion, such that

$$U_A U_{A^c} |\tilde{\psi}\rangle_{AA^c} U_A^{\dagger} U_{A^c}^{\dagger} \approx |\psi\rangle|\chi\rangle,$$
 (4.2)

where $|\psi\rangle$ captures the bulk encoded information while $|\chi\rangle$ is the entanglement mediating erasure correction⁵. This is the case for certain of holographic QECC toy models, such as instances of approximate holographic Bacon-Shor codes[27], (see e.g. Fig. 41 or generally when the skewing is small,) and [24] when imperfectly entangled pairs are used in place of maximally entangled states when building the tensor network. The latter is known to be able to produce the correct single-interval CFT entanglement entropy but fails at the multi-interval level.

The states $|\chi\rangle$ now play the role of the interface tensor in MERA. To leading order, the Rényi entropies associated with $|\chi\rangle$ again scale as the area of the extremal surface where it is explicitly given by the number of entangled states across the bulk cut. Therefore, by (Eq. (3.54)), its magic as measured by the stabilizer Rényi entropy should scale as the area of the RT surface for any additive magic measure as one simply has to count the number of such approximate Bell pairs. Strictly speaking, this again yields an upper bound as we do not optimize over all basis choices.

We also expect this linear dependence between non-local magic and entanglement to extend to non-critical states with translational invariance. For example, it is well-known that the truncated MERA (or more simply an MPS) can describe ground state of gapped

⁵We note that this heuristic argument is only expected to hold approximately in the leading order N for holographic CFTs as that is when they function as approximate erasure correction codes with recovery errors suppressed by 1/N.

phases where entanglement can increase slightly as the system grows, but plateaus at sufficiently large $|A|^6$. The non-local magic again resides on the edges connecting A and B. From the bond counting argument, we again arrives at $\mathcal{M}^{NL} \sim S(A)$ provided \mathcal{M} is an additive measure of magic.

Having established that the non-local magic should scale as the entropy, let's now examine how it should be connected with the anti-flatness of the entanglement spectrum. Consider again the distilled state $|\chi\rangle$ which we represent as an MPS shared between A and B with local magic removed. Recall that since $\chi_A = \operatorname{tr}_B[|\chi\rangle\langle\chi|] = U_A \rho_A U_A^{\dagger}$, their entanglement spectrum and anti-flatness are identical, i.e., $\mathcal{F}(\chi_A) = \mathcal{F}(\rho_A)$.

For simplicity, let's approximate the MPS as entangled states $|\phi\rangle^{\otimes n}$ where each state $|\phi\rangle$ can be thought of as imperfect entangled pairs⁷. These states have volume law entanglement across A and B. We expect this to be a reasonable approximation because MPS with constant bond dimension limits the amount of correlation to be short-ranged, making them close to the tensor products which one can think of as a mean field approximation. We further support this claim with numerical evidence in Appendix D.3.

It is known from [74] that for a typical state $|\phi\rangle_{ab}$ with stabilizer linear entropy $M_{\text{lin}}(|\phi\rangle)$ chosen from its Clifford orbit $\{\Gamma_{ab}|\phi\rangle, \forall \Gamma \in \mathcal{C}_2\}$, the anti-flatness of the entanglement spectrum of $\phi = \text{Tr}_b[|\phi\rangle\langle\phi|]$ when cutting the state in half is given by

$$\mathcal{F}(\phi) = c(d, d_a) M_{\text{lin}}(\phi), \tag{4.3}$$

where $c(d_a, d) = \frac{(d^2 - d_a^2)(d_a^2 - 1)}{(d^2 - 1)(d + 2)}$. Note that the second stabilizer Rényi entropy is related to the stabilizer linear entropy $\mathcal{M}_2 = -\log(1 - M_{\text{lin}})$. Here $M_{\text{lin}} \leq 1 - 2(d + 1)^{-1}$ with d being the dimension of the Hilbert space of $|\phi\rangle$ and $d_a = \sqrt{d}$ the Hilbert space dimension of subsystem a. Applying Eq. (4.3) to each pair, we would have

$$\mathcal{M}_{2}(|\phi\rangle) \approx \frac{\mathcal{F}(\phi_{a})}{c(d, d_{a})}$$

$$\approx -\frac{\operatorname{Pur}(\phi_{a})^{2}}{c(d, d_{a})} \left. \frac{\partial \tilde{S}_{m}(\phi_{a})}{\partial m} \right|_{m=1},$$
(4.4)

where we have applied the approximation Eq. (3.38) to rewrite the R.H.S. in terms of additive anti-flatness measure. Based on the assumption of distillation $|\chi\rangle \approx |\phi\rangle^{\otimes n}$ (See Appendix D.3 for discussion) and additivity of \mathcal{M}_2 we conclude that

$$\mathcal{M}_{2}(|\chi\rangle) \approx n \frac{\operatorname{Pur}(\phi_{a})^{2}}{c(d, d_{a})} |\partial_{m} \tilde{S}_{m}(\phi_{a})||_{m=1}$$

$$= \kappa |\partial_{m} \tilde{S}_{m}(\chi_{A})||_{m=1}.$$
(4.5)

where $\kappa = \text{Pur}(\phi_a)^2/c(d, d_a)$ is some coefficient that depends on the details of $|\phi\rangle$. Note that $\partial_m \tilde{S}_m$ is negative in our convention.

⁶See [101] for example.

⁷For concreteness, one can think of them as imperfect Bell pairs. More generally, they do not have to be qubits, but a pair of qudits that are not maximally entangled.

Since we argued that $\mathcal{M}_2(|\chi\rangle) \approx \mathcal{M}_2^{NL}(|\psi\rangle_{AB})$,

$$\mathcal{M}_{2}^{NL}(|\psi\rangle_{AB}) \approx \kappa |\partial_{m}\tilde{S}_{m}(\chi_{A})||_{m=1}.$$
 (4.6)

for a CFT ground state. Therefore, if one uses the computable stabilizer Rényi entropy \mathcal{M}_2 , we predict that the non-local magic scales linearly with both entanglement entropy and the additive anti-flatness $\partial_m \tilde{S}_m(\chi_A)|_{m=1}$ of the entanglement spectrum across A and B. In Section 4.2, we numerically verify that this is indeed the case for an Ising CFT.

Remark 2. Notably, our reasoning for the area-law scaling of exact magic, i.e. $\mathcal{M}^{(NL)} \sim S(A)$, and the non-flatness relation (4.6) does not rely on any particular properties of the CFT. Indeed, as long as one can concentrate the magic from A to ∂A using the kind of unitary distillation procedure, this area law would also hold for gapped system with entanglement area law. The anti-flatness relation is also similar to the area law scaling of entanglement spread[102].

4.2 Non-local magic in Ising model

In this section we provide numerical computations to support our prior conjectures. We begin with the 1 + 1D transverse field Ising model, with Hamiltonian given by

$$H_{\text{Ising}} = -\cos(\theta) \sum_{i} Z_i Z_{i+1} - \sin(\theta) \sum_{i} X_i. \tag{4.7}$$

We particularly consider Eq. (4.7) near its critical point, when $\theta = \pi/4$.

This model is described by an Ising CFT in the thermodynamic limit at criticality, that is when $\theta = \frac{\pi}{4}$. For our analysis, we perform exact diagonalization to determine the ground state of a 26-site spin chain with periodic boundary condition. Subsequently, the state is partitioned into two contiguous segments: A and \bar{A} . To numerically estimate the non-local magic related to this bipartition, we use the Stabilizer Rényi Entropy measure $\mathcal{M}_2(\{\lambda_i\})$, as defined in Section 3.3.3. Importantly, this measure relies solely on the entanglement spectrum, which we obtain through Singular Value Decomposition (SVD).

At the critical point, we compute the $\mathcal{M}_2(\{\lambda_i\})$ measure while progressively increasing the size of the subsystem |A|. The plot of \mathcal{M}_2 is present in Fig. 4a.

In Fig. 4b, we observe that the non-local magic scales similarly to entropy when we increase the size of the subregion |A|, particularly beyond 3 qubits. This indicates that the non-local magic in the CFT scales logarithmically with |A|, in agreement with our analysis presented in the MERA framework in Section 4.1. Additionally, Fig. 4c demonstrates the proportional relationship between non-local magic and anti-flatness, supporting the estimation in Eq. (4.6).

A similar analysis is applied to study the model away from the critical point, as illustrated in Fig. 5. We define the parameter $g = \theta - \frac{\pi}{4}$, where g quantifies the deviation from criticality. In this regime, we observe that the non-local magic reaches a plateau at a certain point, mirroring the behavior observed in entropy.

In our final analysis, we keep the size of the subregion |A| constant and track the changes in non-local magic as the model approaches and passes through the critical point.

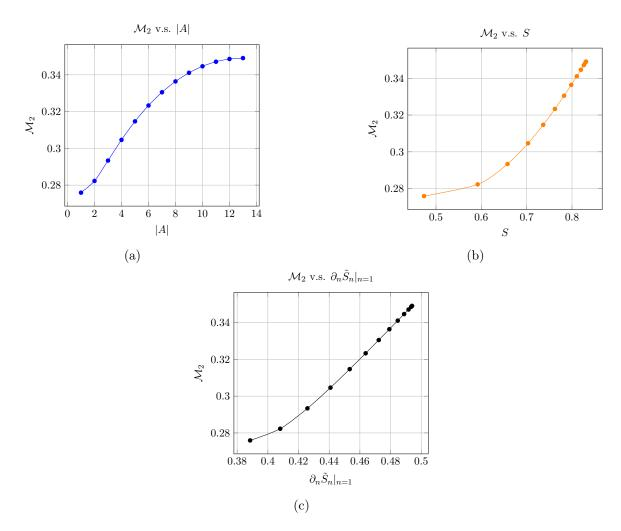


Figure 4: (a) Plot of non-local Stabilizer Rényi Entropy \mathcal{M}_2 v.s. subsystem size |A|; (b) Plot of \mathcal{M}_2 v.s. Entropy S. (c) Plot of \mathcal{M}_2 v.s. the anti-flatness based on entanglement capacity. Model is at critical point, with 26 lattice sites.

As depicted in Fig. 6, a distinct peak in non-local magic is observed. Notably, this peak shifts closer to the critical point (g = 0) and becomes increasingly sharp as the total system size (n) is enlarged. These observations suggest the potential presence of a phase transition in the non-local magic measure. Fig. 7 presents a comparison of non-local magic and antiflatness against the model parameter g, revealing a consistent trend as g changes.

However, it is important to point out that non-local magic is not simply the entanglement entropy despite their similarity in this example. For instance, the ratio between non-local magic and entanglement depends on g. Fig. 8 gives a complete picture of \mathcal{M}_2/S for a 14-qubit Ising chain, as we vary both the parameter g and the subsystem cardinality |A|. We observe that \mathcal{M}_2/S maximizes for angles slightly above the critical point (g=0) due to finite size effect, in agreement with Figs. 6 and 7.

The plateau in Fig. 8 suggests a linear scaling between M_2 and S, as subsystem |A| grows large. As we see that the linear behavior is already apparent at n = 14. Recall from

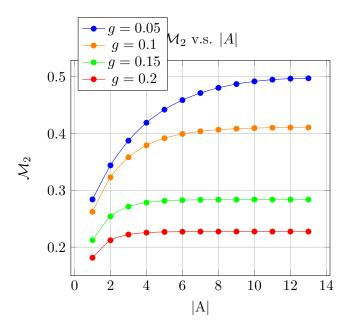


Figure 5: Plot of non-local Stabilizer Rényi Entropy \mathcal{M}_2 v.s. subsystem size |A|. The model parameter $g = \theta - \frac{\pi}{4}$ is adjusted to position the model away from its critical point.

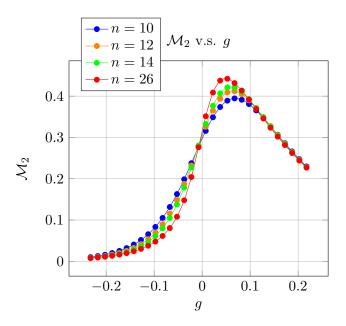


Figure 6: Plot of non-local Stabilizer Rényi Entropy \mathcal{M}_2 v.s. parameter $g = \theta - \frac{\pi}{4}$, at |A| = 5 with increasing total spins n.

the tensor network picture, the linear scaling between non-local magic and entanglement entropy is expected, however, the density of non-local magic can vary depending on the shape of the spectrum. This is reflected in the figure as the asymptotic proportionality constant between M_2 and S depends on θ .

Another instance where non-local magic distinguishes itself from entanglement can be

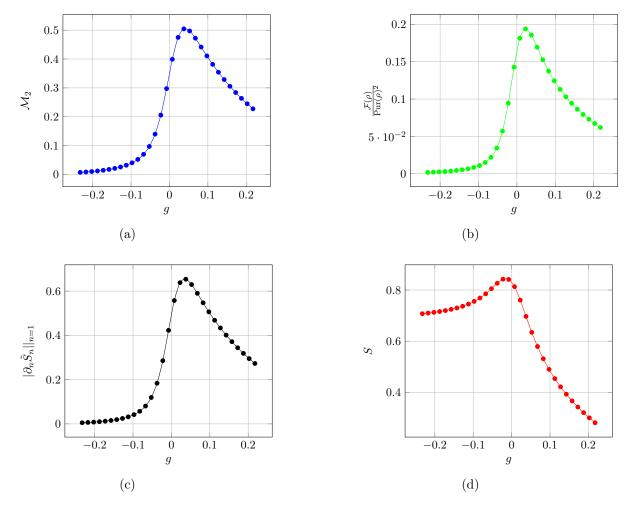


Figure 7: (a) Plot of non-local magic \mathcal{M}_2 v.s. g. (b) Plot of anti-flatness v.s. g. (c) Plot of anti-flatness $|\partial_n \tilde{S}_n|$ v.s. g. (d) Plot of entropy S v.s. g. All of these plots are based on data for fixed subregion size |A| = 13.

found in the context of symmetry breaking. For g < 0, the Ising model enters the symmetry-breaking phase in the thermodynamic limit where the non-local magic further displays a transition. We refer interested readers to Appendix F.1 for details of this discussion.

4.3 Smoothed Magic from Entropic Bounds

However, beyond tensor network and finite-size numerics, we recognize that many of the entropic quantities we have examined so far are generally infinite in conformal field theories and need regularization. It makes more sense to look at smoothed magic, which can be bounded by smoothed max-entropies. On the one hand, it generally leads to finite quantities. On the other hand, for any reasonable simulation of a CFT, it is far more relevant to produce approximations of a target state up to a small precision parameter ϵ instead of the exact state defined by the theory.

In [36], it was shown that under the assumption that the Rényi entropies satisfy $S_n = \frac{s_n}{G_N}$, the smoothed maximal entropy is directly proportional to the following expression:

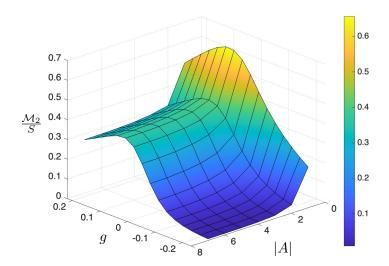


Figure 8: Surface illustrating the ratio of non-local magic to entanglement entropy in n = 14 Ising CFT. We plot \mathcal{M}_2/S as a function of parameter $g = \theta - \pi/4$ and subsystem size |A|. The value \mathcal{M}_2/S reaches a maximum just above criticality (g = 0), before decreasing and ultimately plateauing.

$$S_{max}^{\epsilon} = S + \sqrt{\log \frac{1}{\epsilon} S} + O(c^0), \tag{4.8}$$

where S denotes the von Neumann entropy of the state. A similar expression is obtained by [103] using the explicit spectrum for a 1+1D CFT by Calabrese and Lefevre[104]. This entropy is proportional to the central charge c of holographic CFT, which is assumed to be large. The leading-order correction to this expression is at O(1), making it negligible relative to the primary term.

With this in mind, we can estimate the lower bound for magic as follows:

$$M_{RS}^{(NL,\epsilon)}(\rho_{AA^c}) \ge S_{max}^{\epsilon}(A) - S(A) = \sqrt{S(A)\log\frac{1}{\epsilon}} + O(\epsilon c).$$
 (4.9)

We assume the parameter ϵ to fall within the range $e^{-c} \ll \epsilon \ll c^{-1}$.

Recall that for a given bipartition A and A^c in a holographic CFT, the von Neumann entropy of subregion A to leading order is equal to the area \mathcal{A} of the extremal surface anchored to the entangling boundary ∂A divided by $4G_N$ according to the Ryu-Takayanagi formula[18]. Thus, we can formally represent the lower bound of non-local magic as:

$$M_{RS}^{(NL,\epsilon)}(\rho_{AA^c}) \ge \sqrt{\log \frac{1}{\epsilon}} \sqrt{\frac{\mathcal{A}}{4G_N}},$$
 (4.10)

where G_N denotes the bulk gravitational constant, which is related to the central charge of the CFT through the equation $c = \frac{3R}{2G_N}$ for 1+1 d CFT, and $c \sim \frac{R^{d-1}}{G_N}$ for general dimensions. R is the AdS radius.

Exact and Smoothed Magic in CFTs

Having obtained a lower bound, we now examine the smoothed magic upper bound. Let's pause for a moment and make an interesting observation about exact versus smoothed magic. Consider n copies of $|\psi\rangle = a|00\rangle + b|11\rangle$ which is not maximally entangled. For any additive magic measure, the total magic $M \sim n$. The same can be deduced from the entropy bounds as both the lower and upper bounds pick up a constant multiple of n compared to that of a single copy.

However, smoothed entropies are not additive. If we allow for approximations, then it is known that [105] for any state $|\psi\rangle$ there exist local unitaries $U_A \otimes U_B$ such that

$$F(U_A \otimes U_B | \psi \rangle^{\otimes n}, |\Phi^+\rangle^{S_n - O(\sqrt{n})} \otimes |\chi\rangle) \ge 1 - \epsilon$$
 (4.11)

for some ϵ , where $F(\sigma,\rho)=(\text{Tr}[\sqrt{\sigma^{1/2}\rho\sigma^{1/2}}])^2$ is the Uhlmann fidelity and $|\chi\rangle$ is a state that's entangling $O(\sqrt{n})$ qubits. Because the perfect Bell pairs $|\Phi^+\rangle$ contain zero magic, the smoothed non-local magic of such a system must be upper bounded by $O(\sqrt{n})$ with implicit ϵ dependence. From this, we can derive a tighter upper bound of $O(\sqrt{n}) \sim O(\sqrt{S})$. This agrees with the lower bound up to constant factors. Hence assuming the distillation argument, the smoothed non-local magic $M_{RS}^{(NL,\epsilon)}(\rho_{AA^c}) \sim O(\sqrt{S(A)})$. This is contrasted with magic scaling without smoothing, which has shown to scale linearly with S(A) in tensor networks and small size numerics without smoothing.

A similar argument can be applied to CFTs by taking an n-fold tensor product. Let $|\psi\rangle_{AB}$ now be a CFT ground state with some fixed bipartition. Under such an n-fold tensor product, $c \to nc$ and the magic lower bound scales as $O(\sqrt{c}) \to O(\sqrt{cn})$ where we take identical bipartitions A, B for all copies of the CFT. Although the magic scaling is O(n) according to the smoothed max entropy upper bound, by Eq. (4.11), a tighter bound from Bell pair counting yield $O(\sqrt{n})$ scaling again. On the surface, an n-fold copy of CFTs should have n fold increase of the non-local magic if the measure is additive, however, we see that smoothing in fact always brings about a quadratic reduction in the amount of required magic in producing an approximation of the target state.

It is natural to ask whether the square root scaling of smoothed magic persists for SU(N) gauge theories like holographic CFTs in the large N limit and when the upper/lower bounds in Theorem 4 are tight. Here we conjecture that the lower bound (Eq. (3.59)) is essentially saturated by smoothed magic whereas the non-smoothed magic can scale linearly with the Rényi entropies $S_n(A)$. In other words, the upper bounds (Proposition 5) and (Eq. (3.59)) are approximately saturated up to constant multiplicative factors.

Conjecture 1. Let $|\psi\rangle_{AB}$ be a low energy state of any conformal field theory. Assuming a UV cut off to render entropies finite, let S(A) be the von Neumann entropy of the state on a contiguous subregion A. For any additive measure of magic,

- (a) the smoothed non-local magic evaluated at any fixed precision ϵ is of $O(\sqrt{S(A)})$.
- (b) If the exact non-local magic is well-defined, then it scales as O(S(A)).

A simple reasoning is as follows. Suppose the bipartite entanglement across AB are distillable such that for each Planck area of the RT surface, we can obtain a Bell-like state $|\chi\rangle_{AB}$ which need not be maximally entangled; suppose these states are near identical by the conformal symmetries of the CFT ground state, then we must have O(S(A)) copies of such states. Following a distillation like Eq. (4.11), we obtain at most $O(\sqrt{S})$ states that are imperfectly entangled, in which non-local magic can reside. Note that if no smoothing is allowed, and the magic measure is additive, then the O(S) number of entangled pairs simply contain O(S) amount of magic, consistent with our MERA intuitions and CFT numerics.

This conjecture, if true, has a wider implication for quantum simulations of conformal field theories. Although our naïve expectation is that the non-local magic should increase as the volume of the minimal surface, as indicated by holographic tensor networks, the magic needed to produce a good approximation allows a quadratic reduction. In terms of non-Clifford resources, it implies that an practical preparation of a CFT ground state may permit a quadratic reduction of T gates compared to naïve expectations with moderate scaling with increasing precision ϵ . However, the actual state preparation has to take into account local magic, which is volume law, and multipartite non-local magic, which is not covered by our bipartite analysis. Therefore, although a state isospectral to ρ_A may consume less non-Clifford resource, we make no claim as to how it alters the total resource scaling for the preparation of ρ_A .

Anti-flatness and smoothed magic

Now we comment on a key relation between smoothed magic and entanglement in the CFT. It was suggested in [44] that magic non-locally distributed would be needed to reproduce the anti-flatness of the CFT entanglement spectrum. We have seen a version of it for exact magic in Section 4. We can also verify this relation precisely for smoothed magic — the spectral anti-flatness $\mathcal{F}_R(\rho_A)$ is proportional to the amount of smoothed non-local magic $M_{RS}^{NL}(\rho_{AB})$ to leading order. However, the scaling with entropy is different.

Proposition 7. For any bipartition A and A^c of the CFT ground state, the anti-flatness of the CFT entanglement spectrum necessitates the existence of smoothed non-local magic of at least $O(\sqrt{S(A)\log(1/\epsilon})$. If the distillation argument holds, then

$$\mathcal{F}_R(\rho_A) \sim M_{RS}^{(NL,\epsilon)}(\rho_{AA^c}) = O(\sqrt{S(A)}). \tag{4.12}$$

5 Holographic Magic and Gravity

Heuristically, anti-flatness of the entanglement spectrum is critical in emerging gravity. Various approaches for (entanglement) entropic derivations of the Einstein's equations make use of entanglement first law in both AdS/CFT, e.g.[15, 106–108], and beyond [29–31]. This simple relation connects the stress energy by way of modular Hamiltonian $H_A = -\log \rho_A$. Under a perturbation $\rho_A \to \rho_A + \delta \rho$ such that $\delta S \equiv S(\rho_A + \delta \rho) - S(\rho_A)$ and $\delta \langle H_A \rangle \equiv \text{Tr}[H_A \delta \rho]$, then to linear order $\delta S = \delta \langle H_A \rangle$. As entropy is linked to the area of an extremal surface and H_A can be linked to functions of the stress energy tensor in quantum field theories, $\delta \langle H_A \rangle$ is connected to perturbation in stress energy caused by the perturbation

 $\delta\rho$ while δS can be linked to the area and hence metric perturbation. The combination of these relations produce the Hamiltonian constraint, where a covariantized version leads to the (linearized) Einstein's equations. It is clear that if the spectrum was flat, i.e. the system has zero non-local magic and the modular Hamiltonian is proportional to the identity, then no state perturbation can ever incur entropy and therefore metric perturbations, let alone Einstein gravity. Therefore, it is natural to link non-local magic to the emergence of gravity by way of entanglement spectrum.

In this section, we examine non-local magic in CFTs with dual gravity theories. Although it is speculated that non-local magic should play an important role in the dual theory [39, 44], the precise relation has not been made clear. We now provide a holographic dual of non-local magic: non-local magic in the CFT is backreaction in the bulk.

5.1 Brane tension and magic

Let's make a more precise statement from the point of view of Rényi entropies. Recall that the Rényi entropies in holographic CFTs are computed by the replica geometries which insert a conical singularity that correspond to cosmic branes at various tensions [75, 86]. Therefore, anti-flatness in the entanglement spectrum can be naturally interpreted as the difference between minimal surfaces areas in different backreacted geometries caused by the addition of some stress energy in the form of a cosmic brane with tension \mathcal{T} .

More precisely, the derivative of brane area is related to anti-flatness (Proposition 4),

$$\frac{\partial_n A_n}{4G} = \partial_n \tilde{S}_n. \tag{5.1}$$

The brane tension \mathcal{T} is related to n by

$$\mathcal{T}_n = \frac{n-1}{4nG} \tag{5.2}$$

Hence for n = 1, or tension $\mathcal{T} = 0$, we have that $4G\partial_n A_n|_{n=1} = \partial \mathcal{A}/\partial \mathcal{T}|_{\mathcal{T}=0}$. Applying (Eq. (4.6)) we arrive at a linear relation between $\partial \mathcal{A}/\partial \mathcal{T} \sim \mathcal{M}_2(|\phi\rangle)$, specifically

$$\left| \frac{\partial \mathcal{A}}{\partial \mathcal{T}} \right|_{\mathcal{T}=0} = (4G)^2 |\partial_n \tilde{S}_n||_{n=1} \approx \frac{(4G)^2}{\kappa} \mathcal{M}_2^{NL}(|\psi\rangle_{AB})$$
 (5.3)

which then provides an estimate for the non-local magic $M_{\rm dist}^{(NL)}$ across the bipartition from Theorem 1. Note that the bipartition is arbitrary and each subregion A need not be connected.

That is, non-local magic controls the level of geometric change in response to adding mass energy in the bulk, where the zero magic limit indeed recovers the trivial response function in stabilizer holographic tensor networks. As we showed earlier in Lemma 1, anti-flatness is zero if and only if the non-local magic vanishes. Then, through Section 5.1, there is no back-reaction in the zero magic limit. This is consistent with results from [39].

Remark 3. Recall the flatness problem of the entanglement spectrum is also present in random tensor networks even though they are not stabilizer codes. This is because non-local magic is also low for Haar random states (Remark 1), even though they are not stabilizer codes. Therefore the same type of gravitational backreaction is also "turned off" in [24].

A more rigorous bound relating non-local magic and the Rényi entropy derivatives $\partial_n \mathcal{A}$ can also be proven.

Proposition 8. Assuming the distillation argument where $U_A \otimes U_B |\psi\rangle_{AB} \approx \otimes_i |\phi_i\rangle_{a_ib_i}$ for the state with local magic removed, then the non-local stabilizer Rényi entropy for a CFT under bipartition AB is bounded by

$$\frac{1}{2} \left| \frac{\partial_n \mathcal{A}_n|_{n=2}}{4G} (|\psi\rangle_{AB}) \right| \le \mathcal{M}_2(|\psi\rangle_{AB}) \le \left| \frac{\partial_n \mathcal{A}_n|_{n=1}}{4G} (|\psi\rangle_{AB}) \right| \tag{5.4}$$

See proof in Appendix D.2 and justification of the distillation assumption for CFT in Appendix D.3. We elaborate the regime of validity for various magic bounds and antiflatness relations in Appendix E.

5.2 Magic in Holographic CFT

Note that magic in quantum many-body systems is generally difficult to compute as the cost can grow exponentially with the system size[44, 109]. This scaling is much improved for measures like stabilizer Rényi entropy where the non-linear function of the state can be computed using MPS[47, 110, 111] or enumerator-based tensor networks [112]. However, the computation remains costly at high bond dimensions and for other measures. On the other hand, the bounds of magic from Section 3.3 offer an entropic perspective into this otherwise hard-to-compute quantity by leveraging existing results.

We now study non-local magic in CFTs in light of the general relations derived in Section 3.3. Using the holographic dictionary and applying Conjecture 1, we can predict the behaviour of non-local magic in CFTs that are otherwise difficult to compute. Although the following examples essentially amounts to putting square roots on known holographic entanglement entropies, it is instructive to review their behaviours and analyze their implications for magic and, by extension, classical complexity and quantum resource needed for state preparation. At the same time, holographic calculations enable us to study magic dynamics under quantum quenches, for which existing results have been sparse and size-limited [113] due to prohibitive computational costs.

Static Configurations

We now apply (4.12) to estimate the smoothed non-local magic in the CFT state. To illustrate, consider the thermal state ρ_{AA^c} of a (1+1)d CFT which is purified by B, e.g. in a thermal field double state.

$$|TFD\rangle \propto \sum_{n} \exp(-\beta E_n/2)|E_n\rangle_{AA^c}|E_n\rangle_B$$
 (5.5)

Bipartitioning the system into A and $A^c \cup B$, the behavior of the non-local magic is given by:

$$M_{RS}^{(NL,\epsilon)}(|TFD\rangle_{AA^cB}) \sim \sqrt{\frac{c}{3}\log\left(\frac{\beta}{\pi\delta_{UV}}\sinh\left(\frac{\pi l}{\beta}\right)\right)},$$
 (5.6)

where l is size of subregion A. The magic increases logarithmically with the subregion size l for $l \ll \beta$. However, when the size surpasses the thermal correlation length, represented

by $\beta = \frac{1}{T}$, it becomes proportional to \sqrt{l} . A similar result holds for a small subsystem A of a pure state $|\psi\rangle_{AA^c}$ with that thermalizes under ETH such that A has fixed temperature $T = 1/\beta$.

Now instead consider the bipartition of the system in to AA^c and B. It is known that for holographic CFTs, the system undergoes a confinement-deconfinement phase transition which corresponds to the Hawking-Page transition in the bulk at a critical temperature T_c^8 .

It is known that

$$S(B) = S(AA^c) \sim \begin{cases} O(N^0) & T < T_c \\ O(N^2) & T > T_c \end{cases}$$
 (5.7)

In the same way, we predict a magic phase transition where $M_{RS}^{(NL,\epsilon)}/N$ is discontinuous across T_c in the $N \to \infty$ limit.

Local quench

In the following sections, we consider several time-dependent scenarios and analyze their implications on the system dynamics.

For our first scenario, let's examine a CFT ground state that's been perturbed by a smeared local operator $O_{\alpha}(x,0)$ at t=0. This is then subjected to time evolution governed by the CFT Hamiltonian. We can express the state as:

$$|\psi(t)\rangle = \mathcal{N}e^{-iHt}e^{-\delta H}O_{\alpha}(x,t)|\Omega\rangle.$$
 (5.8)

In the corresponding bulk dual, this equates to introducing an in-falling particle with mass m into the initially vacuum AdS spacetime. The energy-momentum tensor for this scenario can be characterized as:

$$T_{uu} = \frac{mR\alpha^2}{8\pi(u^2 + \alpha^2)^2}. (5.9)$$

Here, α denotes the size of the smeared operator. As α approaches 0, this converges to a delta function in u. The subsequent effect on the bulk spacetime is encapsulated by a shock-wave geometry, as illustrated below in Fig. (9).

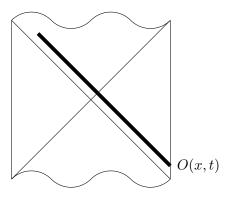


Figure 9: Penrose diagram depicting a shock wave in global coordinates.

⁸This is a simplified account of the transition, which for different theories there can be different phases as one dial up the temperature [114].

We aim to investigate the non-local magic of subsystem A in relation to A^c . These subsystems are separated by the boundary $\partial A = \partial A^c$, a d-2 sphere of radius l. By solving the Einstein equation, [115] derived the leading-order change in entanglement entropy due to the injected energy. Specifically, for a (1+1)d holographic CFT, this change is expressed as:

$$\Delta S(t) = \frac{2mRl\alpha + mR(l^2 - \alpha^2 - t^2)\arctan(\frac{2\alpha l}{t^2 + \alpha^2 - l^2})}{8l\alpha} + O\left((mR)^2\right). \tag{5.10}$$

We can then employ the lower bound to estimate the growth of the non-local magic as follows:

$$M_{RS}^{(NL)}(|\psi(t)\rangle) \sim \sqrt{S(0) + \Delta S(t)}$$

$$\approx \sqrt{S(0)} + \frac{1}{2} \frac{\Delta S(t)}{\sqrt{S(0)}}.$$
(5.11)

In the early-time regime, $t \ll \sqrt{l^2 - \alpha^2}$, the magic exhibits quadratic growth with time, independent of the spacetime dimension. This can be expressed as:

$$\Delta M_{RS}^{(NL)}(t) \sim \kappa_d \frac{mR}{\sqrt{S_0}} \left(\frac{\alpha l}{l^2 - \alpha^2}\right)^2 \frac{t^2}{l^2 - \alpha^2} + O\left(\frac{t^4}{(l^2 - \alpha^2)^2}\right). \tag{5.12}$$

At $t = \sqrt{l^2 - \alpha^2}$, the magic reaches its peak value of $\Delta M_{RS}^{(NL)} = \kappa_d \frac{mR}{\sqrt{S_0}}$, after which it declines to zero. In the long-term regime, it decays following a power-law pattern:

$$\Delta M_{RS}^{(NL)}(t) \sim \frac{mR}{\sqrt{S_0}} \left(\frac{\alpha l}{t^2}\right)^d \left(1 + O\left(\frac{l^2 - \alpha^2}{t^2}\right)\right). \tag{5.13}$$

For the (1+1)d CFT, another intriguing scenario arises when subsystem A encompasses half of the space, signifying $l \to \infty$. In this context, there exists a range in which the magic grows logarithmically with t [116], specifically when $l \ll t \ll D^{1/mR}\alpha$,

$$\Delta M_{RS}^{(NL)}(t) \sim \frac{mR}{\sqrt{S_0}} \log \frac{t}{\alpha},\tag{5.14}$$

where D is quantum dimension of the quench operator O. The value reaches a constant late-time limit of $\Delta M_{RS}^{(NL)} = \frac{\log D}{\sqrt{S_0}}$. This logarithmic growth can only be observed in system with large central charge due to the otherwise small value of D. Note that holographic methods are at a distinct advantage here because magic dynamics for large systems over long periods of time is numerically intractable using existing methods.

Global Quench

We also explore the global quench scenario wherein the perturbation isn't confined to a localized region but influences the entire CFT state. Within the bulk dual, this corresponds to a spherically symmetric in-falling mass shell.

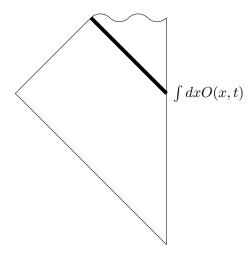


Figure 10: Vaidya geometry. Right side boundary denotes the asymptotic boundary of the AdS-Vaidya spacetime. Outside the mass shell is the black hole geometry. Inside the mass shell is Vacuum AdS in Poincaré patch.

The geometry impacted by the mass shell is characterized by the Vaidya metric. This is essentially the integration of pure AdS with an AdS-Schwarzschild black hole, aligned along the mass shell, as illustrated in Fig. 10.

The shell's descent into the bulk parallels the boundary CFT's thermalization following the global perturbation. The state transitions from the ground state and progressively thermalizes to a certain finite temperature. The entanglement entropy of subregion A serves as a quantitative measure, increasing during this process. Correspondingly, in the bulk perspective, this entropy surge is represented by the expanding area of the minimal surface anchored to the boundary of A.

In a (1+1)-dimensional CFT, it's feasible to precisely solve for the minimal surface [117]. The entropy at t=0 is equivalent to the CFT ground state entropy, given by $S(0)=\frac{c}{3}\log\frac{l}{\delta_{UV}}$. This aligns with the length of the geodesic fully contained within the pure AdS. Following the onset of the quench, the geodesic begins to intersect with the infalling mass shell, causing its length to increase over time. Initially, this growth is quadratic with respect to t,

$$\mathcal{L}(t) = 2\log\frac{l}{\delta_{UV}} + 2\frac{\pi^2 t^2}{\beta^2} + O(t^3). \tag{5.15}$$

As thermalization progresses, the geodesic's intersection with the mass shell delves deeper into the bulk. Once the subregion completes its thermalization at time $t = \frac{l}{2}$, the geodesic no longer intersects the in-falling shell, stabilizing its length to an equilibrium value,

$$\mathcal{L}(t > \frac{l}{2}) = 2\log\frac{\beta}{\pi\delta_{UV}}\sinh\frac{\pi l}{\beta}.$$
 (5.16)

We also detail the behavior of the geodesic length in the late stages, prior to reaching

full thermalization, as outlined below:

$$\mathcal{L}(t \lesssim \frac{l}{2}) = 2\log\left(\frac{\beta}{\pi\delta_{UV}}\sinh\frac{\pi l}{\beta}\right) - \frac{2}{3}\sqrt{2\tanh\frac{\pi l}{\beta}}\left(\frac{l}{2} - t\right)^{\frac{3}{2}} + O\left(\left(\frac{l}{2} - t\right)^{2}\right). \quad (5.17)$$

Based on the aforementioned results, the evolution of the smoothed non-local magic for a subregion in a 2d CFT can be characterized as follows: it increases according to,

$$M_{RS}^{(NL,\epsilon)}(t) \sim \sqrt{c |\log \epsilon|} \left(\sqrt{S_0/c} + \frac{\pi^2 t^2}{6\sqrt{S_0/c}} + O(t^3) \right),$$
 (5.18)

during the initial stages, and as,

$$M_{RS}^{(NL,\epsilon)}(t) \sim \sqrt{c \left|\log \epsilon\right|} \left(\sqrt{S_T/c} - \frac{1}{18} \frac{\sqrt{2 \tanh \frac{\pi l}{\beta}}}{\sqrt{S_T/c}} \left(\frac{l}{2} - t \right)^{\frac{3}{2}} + O\left(\left(\frac{l}{2} - t \right)^2 \right) \right), \quad (5.19)$$

during the latter phases when the subregion is nearing full thermalization. This can be contrasted with the dynamics of total subsystem magic under thermalization[113] which decays after a quick initial rise.

Wormhole

Lastly, we examine a thermalization process involving two copies of CFT states. This dynamic process corresponds to the evolution of an expanding wormhole in the bulk dual.

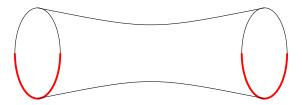


Figure 11: Wormhole geometry

Let us revisit the thermal-field-double (TFD),

$$|\text{TFD}\rangle = \frac{1}{\sqrt{Z(\beta)}} \sum_{n} e^{-(\frac{\beta}{2} + 2it)E_n} |E_n\rangle_L |E_n\rangle_R$$
 (5.20)

We designate our region of interest to encompass a section from both the left and right CFT states (illustrated in Fig. 11). The entanglement entropy of this composite region is probed by the extremal surface spanning the wormhole, connecting the left and right segments.

In this setup, we assume symmetry when exchanging the two CFT sides. Specifically, we mandate that the subregion A on one side mirrors its counterpart on the other side. See red region in Fig. 11. Given this symmetry, the extremal surface occupies a plane defined by constant transverse spatial coordinates and is characterized solely by the relationship between time and the radial direction.

At the boundary time t = 0, the area of extremal surface is given by

$$\mathcal{A}(0) = \frac{\beta r_{\infty}}{\pi} V_{d-2}.\tag{5.21}$$

where r_{∞} is the UV cutoff of radial coordinates. This extremal area is proportional to the volume of subregion boundary ∂A , reminiscent of the area law entanglement observed in gapped systems. As time progresses, the extremal surface accrues additional contributions from regions beyond the horizon. As highlighted in [118], this contribution exhibits a straightforward linear relationship with the boundary time, as illustrated below:

$$\mathcal{A}(t) = \frac{4\pi t}{\beta} \alpha_d V_{d-2}, \quad \text{for } t \gg \beta.$$
 (5.22)

The linear growth eventually ceases when the extremal surface traversing the wormhole is surpassed by another, more minimal configuration. A different set of competing extremal surfaces, anchored to the same entangling boundary but bypassing the wormhole, emerges. These surfaces are essentially combinations of the extremal surfaces corresponding to subregions within each individual thermal CFT. Their area is given by

$$\mathcal{A}(\infty) - \mathcal{A}(0) = \frac{2\pi}{\beta} V_{d-1}.$$
 (5.23)

The transition of dominant extremal surface occurs around $t \sim R$, which corresponds to the size of the subregion under consideration. Consequently, we anticipate the non-local magic in this TFD state to scale as follows:

$$M_{RS}^{(NL,\epsilon)}(t) \sim \sqrt{|\log \epsilon|} \sqrt{S_0 + \frac{4\pi t}{\beta} \alpha_d V_{d-2}}, \quad \text{for } \beta \ll t < R$$

$$\sim \sqrt{|\log \epsilon| S_T}, \quad \text{for } t \ge R.$$
(5.24)

6 Discussion

In this work, we explored the question: what dual boundary quantity enables gravitational back-reaction in the bulk? The celebrated formula of Ryu and Takayanagi provides a fundamental observation of the AdS-CFT conjecture by showing that areas in AdS correspond to entanglement entropies in the CFT. In the greater context of spacetime and gravity emerging from quantum information, we ask: If entanglement builds geometry, then what builds gravity? In this work we show that the strength of gravitational back-reaction is connected to (non-local) magic in CFT. In other words, gravity is magical! Accordingly, both defining properties of quantumness admit holographic counterparts in AdS.

To obtain this result, we studied the interplay between non-local magic and entanglement. We show that for any quantum state in a finite dimensional Hilbert space, this form of non-stabilizerness that can only live in the bipartite correlations is lower bounded by the anti-flatness of the entanglement spectrum and upper bounded by the amount of entanglement in the system as defined by Rényi entropies. We then apply these results to CFTs and conclude that both the exact and smoothed non-local magic is proportional to

various notions of anti-flatness. However, they scale differently with entropy — the exact non-local magic scales linearly with the von Neumann entropy of a CFT subregion while the smoothed magic only scales as the square root. Numerically we verify that non-local magic is sensitive to quantum phase transition in a way that is different from entanglement. We also examined its behaviour under symmetry breaking.

Finally, in the context of holographic CFTs, we derive a quantitative relation between non-local magic and the level of gravitational back-reaction. Using the bulk gravity theory, smoothed non-local magic in the CFT can also be estimated holographically. As non-stabilizerness in quantum systems are generically hard to compute, our work also provides an important estimate on the practical level and constrain magic distributions using existing data and well-founded methods like tensor networks and DMRG.

There are several directions that are of interest for future work. The key constraints for non-local magic here are given in terms of inequalities. Part of the reason for bounds instead of a precise equality is that non-local magic requires extremization while the computation of magic itself is already non-trivial. However, given the universal behaviour of non-local magic across multiple distinct measures of anti-flatness, there is reason to believe that a unifying statement or even a precise equality exists between entanglement spectral properties and magic. In the particular case of quantum field theory, it is also crucial to generalize our observations to definitions of magic that is native to the infinite dimensional system, e.g. non-Gaussianity, as well as other different measures of spectral anti-flatness.

Approaching non-local magic from a different perspective, we can start with state ρ_A from the usual stabilizer polytope and construct a purified state ψ_{AB} . One can also define a non-local magic as the minimal magic among all possible purifications. In the same vein of connecting magic with entanglement, we ask whether it is possible to define instead magical entanglement, i.e., the entanglement that cannot be removed by any Clifford operation⁹. In this case, one can easily show from our entropy bounds that magical entanglement is an upper bound of non-local magic. However, it is yet unknown whether the two definitions are equivalent. Finally, recall that non-local magic can be generalized to systems with multi-partite entanglement. This will be crucial in understanding the behaviour of e.g. Haar random states, random tensor networks, and holographic states. As the type of multi-partite entanglement is quite constrained for stabilizer states, non-local magic may be crucial in the classification of multi-partite entanglement.

For CFTs specifically, several of our results rely on the assumption that the bipartite entanglement across a subregion A and its complement B in a pure state can be approximately converted into a tensor product of entangled pairs through unitaries that only act on the respective subregions. Although this assumption is well-supported by numerics and well-motivated by holographic tensor networks models, it is unclear the extent to which this holds for a single copy of (holographic) CFT in general. This assumption may also admit further modification in the case where A consists of multiple disjoint regions. It is important that we understand the regime of validity for such assumptions and pave the way for proving Conjecture 1 and extending the generality of Proposition 7.

⁹We thank Kaifeng Bu for this suggestion.

Just like various types of entanglement can admit different holographic interpretations, a similar situation may hold for magic. Although we take a first step towards addressing the open question of what is the holographic dual of magic, much remains unknown. For instance, the connection we identify with anti-flatness signals a link between non-local magic and gravitational back-reaction. However, because we lack a systematic understanding of how the bulk duals should deform under a sequence of boundary theories that have increasing flat spectrum, the physical meaning of how the removal of magic turns off backreaction is unclear. Additionally, it is possible that other gravitational phenomena generating backreaction have a different magical origin on the boundary. If that is the case, we eventually wish to distinguish them from the consequence of bipartite non-local magic in the boundary theory.

Although it has been suggested that boundary states with flat entanglement spectrum are dual to peculiar bulk states of fixed areas[119, 120], exactly how these bulk states should be interpreted holographically remains to be understood. To this end, a more precise relation between magic and emergent gravity [20] in the bulk, one which does not rely on the distillation assumptions used in this work, is highly desirable. Furthermore, a connection between magic and a local function of curvature generated by more physical forms of stress energy instead of an extended conical singularity such as a cosmic brane may provide a more natural link with the Einstein's equations or the Hamiltonian constraint. A more comprehensive understanding of holographic magic through the lens of dynamics such as quantum chaos[48] and (classical) complexity can also provide another unique perspective that is not captured by our current work.

More broadly, this work calls for several important lines of investigation as we move towards establishing non-local magic as a key metric for characterizing quantum many-body systems. For instance, the tensor product of random single-qubit states, the ground states of physical quantum many-body systems, and the Haar random states all have volume law magic scaling. Purely from the point of view of entanglement entropy, they can also be mimicked by stabilizer states. However, their non-local magic behaves very differently. Thus it provides a distinct indicator for the properties of the underlying quantum systems that are invisible to entanglement entropy or total non-stabilizerness alone. It would also be intriguing to study the role of non-local magic in quantum phase transition, in symmetry breaking, and in non-equilibrium systems.

Acknowledgments

We would like to thank Chris Akers, Vijay Balasubramanian, Ning Bao, Ed Barnes, Kaifeng Bu, Xi Dong, Sophia Economou, Monica Kang, Cynthia Keeler, Nick Mayhall, Jason Pollack, Howard Schnitzer, Brian Swingle, Christopher White, Tianci Zhou for helpful comments, resource, and discussions. We are especially grateful to Christopher White and Daniele Iannotti for identifying the mistakes in the earlier version of this manuscript. C.C. and A.H. would like to thank the organizers of the Quantum Information and Quantum Matter Conference at NYU Abu Dhabi during which this work was first conceived. C.C. acknowledges the support by the Air Force Office of Scientific Research (FA9550-19-1-0360),

the National Science Foundation (PHY-1733907), and the Commonwealth Cyber Initiative. The Institute for Quantum Information and Matter is an NSF Physics Frontiers Center. AH acknowledges support from PNRR MUR project PE0000023-NQSTI and PNRR MUR project CN 00000013 -ICSC. W.M. is supported by the U.S. Department of Energy under grant number DE-SC0019470, and by the Heising-Simons Foundation "Observational Signatures of Quantum Gravity" collaboration grant 2021-2818. S.F.E.O. acknowledges support from PNRR MUR project PE0000023-NQSTI. L.L. is funded through the Munich Quantum Valley project (MQV-K8) by Bayerisches Staatsministerium für Wissenschaft und Kunst and DFG (CRC 183).

A Invariance of STAB₀

In this section, we prove that STAB₀ is invariant under the following operations

- 1. Clifford unitaries. $\rho \to U \rho U^{\dagger}$ with $U \in \mathcal{C}(d^n)$.
- 2. Composition with stabilizer states, $\rho \to \rho \otimes \sigma$ with σ a stabilizer state.
- 3. Partial trace of the first qudit, $\rho \to \text{Tr}_1(\rho)$
- 4. Computational basis measurement on the first qudit, $\rho \to (|i\rangle\langle i| \otimes \mathbb{1}_{n-1})\rho(|i\rangle\langle i| \otimes \mathbb{1}_{n-1})/\mathrm{Tr}(\rho|i\rangle\langle i| \otimes \mathbb{1}_{n-1})$ with probability $\mathrm{Tr}(\rho|i\rangle\langle i| \otimes \mathbb{1}_{n-1})$

Proposition 9. Clifford Invariance. Given $\sigma \in STAB_0$ and $C \in C(d^n)$, then $C\sigma C^{\dagger} \in STAB_0$

Proof.

$$C\sigma C^{\dagger} = \frac{1}{d^n} \sum_{P \in G} CPC^{\dagger} = \frac{1}{d} \sum_{\tilde{P} \in \tilde{G}} \tilde{P}$$
 (A.1)

the latter is an element of STAB₀ since it is the equal-weighted sum of Pauli operators of a commuting set. This is since $C: P \mapsto \tilde{P} \in \tilde{\mathcal{P}}$ and the action of a unitary on a subgroup G does not modify the commutation relations.

Proposition 10. Given $\rho \in STAB_0$ and $\tau \in STAB_0$ then $\rho \otimes \tau \in STAB_0$

Proof.

$$\rho \otimes \sigma = \frac{1}{d^{2n}} \sum_{P \in G_1, Q \in G_2} P \otimes Q = \frac{1}{d^2} \sum_{P \otimes Q \in G_1 \times G_2} P \otimes Q. \tag{A.2}$$

where the latter is an element of STAB₀ since the tensor product of Pauli operators is still a Pauli operator and the Cartesian product of a group is still a group, and since the tensor product does not affect the commutation relations of the G_1 or G_2 , then $G_1 \times G_2$ is a commuting group and so $\rho \otimes \sigma \in STAB_0$.

Proposition 11. Given a state $\rho \in STAB_0$ then $Tr_1\rho \in STAB_0$

$$\operatorname{Tr}_{1}(\rho) = \frac{1}{d^{n}} \sum_{P \in G} \operatorname{Tr}(P_{1}) P_{2...n} = \frac{1}{d^{n-1}} \sum_{P_{2...n} \in \operatorname{Tr}_{1}(G)} P_{2...n}$$
(A.3)

where P_1 labels the Pauli operator on the first qudit of P. It is easy to observe that the only elements whose partial trace is different from 0 are the ones with $P_1 = 1$. These elements that were in G are still commuting Pauli operator in the traced group Tr_1G .

Proposition 12. Given a state ρ and $\{|i\rangle\}$ the 1-qudit computational basis, then $(|i\rangle\langle i|\otimes i)$ $\mathbb{1}_{n-1}$) $\rho(|i\rangle\langle i|\otimes\mathbb{1}_{n-1})/\mathrm{Tr}(\rho|i\rangle\langle i|\otimes\mathbb{1}_{n-1})\in\mathrm{STAB}_0$

Proof. For the sake of simplicity, let us consider the case for a multi-qubit system and i = 0, it can be easily generalized for $i \neq 0$ and qudits.

$$\frac{(|0\rangle\langle 0| \otimes \mathbb{1}_{n-1})\rho(|0\rangle\langle 0| \otimes \mathbb{1}_{n-1})}{\operatorname{Tr}(\rho|0\rangle\langle 0| \otimes \mathbb{1}_{n-1})} = \frac{\sum_{P \in G} \operatorname{Tr}(|0\rangle\langle 0|P_1)|0\rangle\langle 0| \otimes P_{2\dots n}}{\sum_{P \in G} \operatorname{Tr}(|0\rangle\langle 0|P_1)\operatorname{Tr}(P_{2\dots n})}$$
(A.4)

$$= \frac{1}{2^{n-1}} \frac{\sum_{P \in G} \operatorname{Tr}(P_1|0\rangle\langle 0|)|0\rangle\langle 0| \otimes P_{2\dots n}}{\sum_{P_1 \in \operatorname{Tr}_{2\dots n}G} \operatorname{Tr}(P_1|0\rangle\langle 0|)}$$
(A.5)

$$= \frac{1}{2^{n-1}} \frac{\sum_{P \in G|P_1 \in \{1,Z\}} |0\rangle\langle 0| \otimes P_{2...n}}{\sum_{P_1 \in 1,Z \cap \text{Tr}_{2...n}G}}$$

$$= |0\rangle\langle 0| \otimes \frac{1}{2^{n-1}} \frac{\sum_{P \in G|P_1 \in \{1,Z\}} P_{2...n}}{\sum_{P_1 \in 1,Z \cap \text{Tr}_{2...n}G}}$$
(A.6)

$$= |0\rangle\langle 0| \otimes \frac{1}{2^{n-1}} \frac{\sum_{P \in G \mid P_1 \in \{1,Z\}} P_{2...n}}{\sum_{P_1 \in 1,Z \cap \text{Tr}_{2..n} G}}$$
(A.7)

(A.8)

note that $\sum_{P_1 \in \mathbb{I}, Z \cap \text{Tr}_{2...n}G}$ can be either 1 or 2, due to the terms $\mathbb{I}_n Z \mathbb{I}_{n-1}$. While on the numerator the only terms surviving have on the first qubit 1 or Z. Now it is not difficult to see that for G to be a commuting group if $\sum_{P_1 \in \mathbb{I}, Z \cap \text{Tr}_{2...n}G} = 1$ then there will be no multiplying factor to the numerator, while in the other case, there will be a 2 since each non-zero $P_{2...n}$ has to repeat twice. Then it is not difficult to see that one has a stabilizer state, because $P_{2...n}$ is still summing on a commuting Pauli subgroup.

Prof of Proposition 3

Proof. Let us start by expanding the relative entropy, we have

$$\mathcal{F}_R(\rho) = -\min_{\sigma \in \text{FLAT}^{(n)}} \text{Tr}[\rho \log \sigma] - S(\rho). \tag{A.9}$$

Since the elements of FLAT are all proportional to projection operators, it is possible to choose σ such that $\sigma = \mathbb{1}_r/r \oplus 0_{d-r}$ is diagonal in the same basis as ρ where $r \equiv \operatorname{rank}(\rho)$, $\mathbb{1}_r$ is the identity on a subspace of dimension r, and 0_{d-r} is the zero-matrix of dimension $(d-r)\times(d-r)$. Hence the first term becomes $\log r\operatorname{Tr}\rho=\log r=S_{max}(\rho)$ and $\mathcal{F}_R(\rho)\leq$ $S_{max}(\rho) - S(\rho)$.

To show that the minimum is attained for a rank r density operator ρ when $\mathcal{F}_R(\rho) =$ $S_{max}(\rho) - S(\rho)$, suppose on the contrary that there exists $\sigma = \Pi_k/k$, where Π_k is a projection operator of rank k such that the first term is less than $\log r$ and making $\mathcal{F}_R(\rho) < S_{\max}(\rho) - 1$ $S(\rho)$. Let $M = \rho \log \sigma$; in the diagonal basis of σ , where we denote the diagonal element by λ_i , one has

$$\operatorname{Tr} M = \sum_{i} M_{ii} = \sum_{i} \rho_{ij} \delta_{ji} \log \lambda_{i} = \sum_{i} \rho_{ii} \log \lambda_{i}. \tag{A.10}$$

Let us note that when i > k, $\log \lambda_{i>k} = -\infty$. Then in order for the trace of $M = \rho \log \sigma$ to be finite, we need $\rho_{ii} = 0$ for any $\lambda_i \neq 0$ to be 0. On the other hand, we know that if the diagonal of a positive semi-definite matrix has a zero on the diagonal, then the corresponding rows and columns must be all 0s. Then it implies that up to rearranging the rows and columns for the sake of clarity,

$$\rho = \begin{pmatrix} A & 0 \\ 0 & 0 \end{pmatrix} \tag{A.11}$$

where A is a $k \times k$ block matrix of rank at most k. Therefore, $-\text{Tr}M = \log k \, \text{Tr}[AI] = \log k < \log r$ by assumption, we must have k < r. Because dim $A \ge \text{rank}(A)$, it follows that $\text{rank}(A) = \text{rank}(\rho) \le k < r$, which is a contradiction.

B Proof of Theorem 1

In this section, we prove Theorem 1. Let us start from the upper bound. Being defined through two minima, we can arbitrarily choose a state ψ and a stabilizer σ to upper bound $M_{\mathrm{dist}}^{(NL)}$. Consider the state $|\psi_{AB}\rangle$, whose Schmidt decomposition can be written as $|\psi_{AB}\rangle = \sum_{i}^{D} \lambda_{i} |\lambda_{i}^{A} \lambda_{i}^{B}\rangle$, where λ_{i} are the Schmidt coefficients and D its Schmidt rank. Due to the minimization over $U = U_{A} \otimes U_{B}$, the basis $|\lambda_{i}^{A/B}\rangle$ can be brought in the computational basis (or another complete stabilizer basis)

$$U|\lambda_i^{A/B}\rangle = |s_i^{A/B}\rangle \tag{B.1}$$

Then, we choose $|\sigma\rangle = \sum_i^{d^{\lfloor \log_d D \rfloor}} \frac{1}{d^{\lfloor \log_d D \rfloor/2}} |s_i^A s_i^B\rangle$, where $\lfloor \cdot \rfloor$ labels the floor function. Let us then compute the upper-bound to $M_{\rm dist}^{(NL)}(\psi_{AB})$.

$$M_{\text{dist}}^{(NL)}(\psi_{AB}) \le \frac{1}{2} \left\| \sum_{ij}^{D} \lambda_i \lambda_j |s_i^A s_i^B\rangle \langle s_j^A s_j^B| - \sum_{ij}^{d^{\lfloor \log D \rfloor}} d^{-\lfloor \log_d D \rfloor} |s_i^A s_i^B\rangle \langle s_j^A s_j^B| \right\|$$
(B.2)

$$= \sqrt{1 - \sum_{ij}^{D} \sum_{kl}^{d^{\lfloor \log D \rfloor}} d^{-\lfloor \log D \rfloor} \lambda_i \lambda_j \langle s_l^A s_l^B | s_i^A s_i^B \rangle \langle s_j^A s_j^B | s_k^A s_k^B \rangle}$$
(B.3)

where we first used the Fuchs-Van der Graaf inequality, where the equality comes by ψ_{AB} and σ being pure states, and then rewritten the states in their Schmidt decomposition. Now without loss of generality, since $d^{\lfloor \log_d D \rfloor} \leq D$, due to our degrees of freedom in the choice of σ and ψ_{AB} we can order the basis states such that only the first $d^{\lfloor \log_d D \rfloor}$ have nonzero overlap, and so it follows:

$$M_{\text{dist}}^{(NL)}(\psi_{AB}) \le \sqrt{1 - \sum_{ij}^{d^{\lfloor \log_d D \rfloor}} d^{-\lfloor \log_d D \rfloor} \lambda_i \lambda_j}$$
(B.4)

$$\leq \sqrt{1 - \sum_{ij}^{d^{\lfloor \log_d D \rfloor}} D^{-1} \lambda_i \lambda_j}$$
(B.5)

$$\leq \sqrt{1 - \sum_{i}^{d^{\lfloor \log_d D \rfloor}} D^{-1} \lambda_i^2} \tag{B.6}$$

$$= \sqrt{1 - \frac{1}{D} + \sum_{i=d^{\lfloor \log D \rfloor}}^{D} D^{-1} \lambda_i^2}$$
 (B.7)

$$= \sqrt{1 - \frac{1}{D} + \lambda_{\max}^2 \left(1 - \frac{d^{\lfloor \log_d D \rfloor}}{D}\right)}$$
 (B.8)

$$= \sqrt{1 - e^{S_{max}(A)} + e^{S_{\infty}(A)} \left(1 - \frac{e^{\log d \lfloor S_{max}(A)/\log d \rfloor}}{e^{S_{max}(A)}}\right)}$$
 (B.9)

where we first utilized the inequality $D^{-1} \leq d^{-\log_d D}$, and since $\lambda_i > 0$ by definition, we can upper bound $M_{\text{dist}}^{(NL)}(\psi_{AB})$ by simply considering the diagonal terms. Next, we employed $\sum_i^D \lambda_i^2 = 1$ to rewrite our inequality, and finally, we utilized $S_{\text{max}}(A) = \log D$ and $S_{\infty} = \log \lambda_{\text{max}}^2$.

Let us now focus on the lower bound. To prove it let us first provide a bound between $\mathcal{F}(\psi)$ and $M_{dist}(\psi)$.

Lemma 2. Let ψ be a state then its flatness $\mathcal{F}(\psi)$ is upper bounded by M_{dist} as follows

$$\mathcal{F}(\psi) \le 8M_{dist}(\psi). \tag{B.10}$$

Proof. Starting from the flatness one can add a zero term to it; take a flat state $\sigma \in STAB_0$

$$\mathcal{F}(\psi) = \mathcal{F}(\psi) - \mathcal{F}(\sigma). \tag{B.11}$$

We can then bound the flatness as follows:

$$\mathcal{F}(\psi) = \text{Tr}(\psi^3 - \sigma^3) - \text{Tr}\left((\psi^2)^{\otimes 2} - (\sigma^2)^{\otimes 2}\right)$$
(B.12)

$$= \left| \operatorname{Tr}(\psi^3 - \sigma^3) \right| + \left| \operatorname{Tr} \left((\psi^2)^{\otimes 2} - (\sigma^2)^{\otimes 2} \right) \right| \tag{B.13}$$

$$\leq \left| \operatorname{Tr}(\psi^3 - \sigma^3) \right| + 2 \left| \operatorname{Tr} \left((\psi^2) - (\sigma^2) \right) \right| \tag{B.14}$$

$$\leq 1 - (1 - T)^3 + 2 - 2(1 - T)^2 \leq T^3 + 7T \leq 8T$$
 (B.15)

where $T = 1/2 \|\psi - \sigma\|_1$. In the second line we made use of the triangular inequality, in the third line, we used the following inequality

$$|\operatorname{Tr}(\psi^2)\operatorname{Tr}(\psi^2) - \operatorname{Tr}(\sigma^2)\operatorname{Tr}(\sigma^2)| \le |\operatorname{Tr}(\psi^2)\left(\operatorname{Tr}(\psi^2) - \operatorname{Tr}(\sigma^2)\right)| + |\left(\operatorname{Tr}(\psi^2) - \operatorname{Tr}(\sigma^2)\right)\operatorname{Tr}(\sigma^2)|$$
(B.16)

$$\leq 2|\text{Tr}(\psi^2) - \text{Tr}(\sigma^2)| \tag{B.17}$$

while in the fourth line we used [121, Lemma 1.2] and then $T^3 \leq T$, since $0 \leq T \leq 1$. By minimizing over $\sigma \in STAB$ we prove the lower bound with $M_{dist}(\psi)$.

Using Lemma 2, we can thus write,

$$\mathcal{F}(\psi_A) \le 8 \min_{U_A} M_{\text{dist}}(U_A \psi_A U_A^{\dagger}) \tag{B.18}$$

where $\psi_A = \operatorname{tr}_B \psi_{AB}$ and we used that $\mathcal{F}(\psi_A)$ is invariant under the action of global unitaries. Now, let us show that $\min_{U_A} M_{\operatorname{dist}}(U_A \psi_A U_A^{\dagger}) \leq M_{\operatorname{dist}}^{(NL)}(\psi_{AB})$. First recall that given $\psi_A = \operatorname{Tr}_B(\psi_{AB})$ due to the monotonicity of M_{dist} one has $M_{\operatorname{dist}}(\psi_A) \leq M_{\operatorname{dist}}(\psi_{AB})$. Now let us prove the statement by contradiction. First, let U_A be the unitary attaining the minimum in Eq. Eq. (B.18). Let us suppose that there exists a bipartite unitary $U \equiv V_A \otimes V_B$ obeying

$$M_{\text{dist}}(U_A \psi_A U_A^{\dagger}) > M_{\text{dist}}(U \psi_{AB} U^{\dagger})$$
 (B.19)

Then we have the following chain of inequalities

$$M_{\text{dist}}(U_A \psi_A U_A^{\dagger}) > M_{\text{dist}}(U \psi_{AB} U^{\dagger}) \ge M_{\text{dist}}(\text{tr}_B U \psi_{AB} U^{\dagger}) = M_{\text{dist}}(V_A \psi_A V_A^{\dagger})$$
 (B.20)

and this is a contradiction to the statement that U_A attains the minimum. Therefore, one obtains that $\min_{U_A} M_{\text{dist}}(U_A \psi_A U_A^{\dagger}) \leq M_{\text{dist}}^{(NL)}(\psi_{AB})$. This result combined with Lemma 2 concludes the proof.

C Stabilizer relative entropies

C.1 Proof of Theorem 2

Let us start by proving the upper-bound to $M_{RS}^{(NL)}$. We choose $\sigma_{AB} = \mathbb{1}_{d^{\lceil \log_d D \rceil}}/d^{\lceil \log_d D \rceil} \oplus 0_{n-\lceil \log_d D \rceil}$ where D is the Schmidt rank of ρ_A . Then expanding the relative entropy expansion one obtains the following bound

$$M_{RS}^{(NL)}(\psi_{AB}) \le -\text{Tr}[\psi_{AB}\log\sigma_{AB}] = \text{Tr}[\sum_{i,j=1}^{D} \lambda_i \lambda_j |s_i\rangle\langle s_j| \sum_{k=1}^{d^{\lceil \log_d D \rceil}} |s_k\rangle\langle s_k| \log d\lceil \log_d D\rceil]$$
(C.1)

$$= \lceil \log_d D \rceil \log d \operatorname{Tr}[\psi_{AB}] = \log d \lceil S_{max}(A) / \log d \rceil, \tag{C.2}$$

Concluding the proof for the upper bound. Shifting our focus on the lower bound instead, let us note that for any ρ , $M_{RS}(\rho) \geq \mathcal{F}(\rho)$. This is a simple consequence of $STAB_0^{(n)} \subset FLAT^{(n)}$. Because $\mathcal{F}(\rho)$ is isospectral under any unitary conjugation, it must follow that $M_{RS}(U\rho U^{\dagger}) \geq F(U\rho U^{\dagger}) = F(\rho)$. Therefore,

$$\mathcal{F}_R(\rho_A) \le \min_{U_A} M_{RS}(U_A \rho_A U_A^{\dagger}). \tag{C.3}$$

On the other hand, for any ρ_A , from monotonicity it follows that $M_{RS}(\rho_{AB}) \geq M_{RS}(\rho_A)$ where $\rho_A = \text{Tr}_B[\rho_{AB}]$. Therefore, we must have

$$\min_{U_A} M_{RS}(U_A \rho_A U_A^{\dagger}) \le \min_{U = V_A \otimes V_B} M_{RS}(U \rho_{AB} U^{\dagger}) \equiv M_{RS}^{(NL)}(\rho_{AB}). \tag{C.4}$$

We can see that this is true from a proof by contradiction. Suppose there exists some U_A, U which attains the respective minima but has

$$M_{RS}(U_A \rho_A U_A^{\dagger}) > M_{RS}(U \rho_{AB} U^{\dagger}),$$

then from monotonicity, we must have

$$M_{RS}(U_A \rho_A U_A^{\dagger}) > M_{RS}(U \rho_{AB} U^{\dagger}) \ge M_{RS}(\operatorname{Tr}_B[U \rho_{AB} U^{\dagger}]) = M_{RS}(V_A \rho_A V_A^{\dagger})$$

for some local unitary V_A which yields a lower distance than U_A . Since we assumed that U_A attains the minimum, this violates our assumption, concluding the proof for the lower bound.

C.2 Proof of Proposition 5

To bound the non-local magic of a pure state ρ_{AB} , consider a pure state $\psi_{AB} = U\rho_{AB}U^{\dagger}$ where $U = U_A \otimes U_B$ and ψ_A , ψ_B are isospectral (up to truncation of 0 eigenvalues) to that of a subsystem ρ_A , ρ_B . Suppose they are states where we have removed the local magic such that both ψ_A , ψ_B are diagonal in the computational (or another complete stabilizer basis). Again, this can be done by first rewriting the state ρ_{AB} in the Schmidt basis, which is orthonormal. Then we replace the Schmidt basis with an orthonormal stabilizer basis to get ψ_{AB} . Since the mixture of stabilizer states is in the convex hull of stabilizer states, each ψ_A , ψ_B must have zero local magic. Note that there are also other basis choices such that the basis state need not be a stabilizer, such states can also be in the convex hull of the stabilizer group as long as they are not pure states.

By definition, $M_R^{(NL)}(\psi_{AB}) \leq M_R(\psi_{AB})$ because we have chosen a particular instance of the local unitary $U_A \otimes U_B$ on the right hand side whereas the left hand side is minimized over all possible instances. Now we evaluate the relative entropy of magic $M_R(\psi_{AB}) = -S(\psi_{AB}) - \min_{\sigma \in \text{STAB}} \text{Tr}[\psi_{AB} \log \sigma_{AB}]$. Since ψ_{AB} is pure, $S(\psi_{AB}) = 0$. If σ_{AB} is pure, then the relative entropy is either 0 when $\sigma = \psi$ or ∞ for any other σ that's mixed.

We pick a stabilizer state $\sigma_{AB} = \sum_i \lambda_i^2 |s_i\rangle \langle s_i|_{AB}$ where λ_i are the Schmidt coefficients of $\psi_{AB} = \sum_i \lambda_i |s_i\rangle_{AB}$ where $|s_i\rangle$ are the stabilizer basis we chose. Then for the second term, we write

$$M_R(\psi_{AB}) = -\text{Tr}[\psi_{AB}\log\sigma_{AB}] \tag{C.5}$$

$$= -\text{Tr}\left[\sum_{ij} \lambda_i \lambda_j |s_i\rangle \langle s_j| \sum_k \log(\lambda_k^2) |s_k\rangle \langle s_k|\right]$$
 (C.6)

$$= -\sum_{i,i,k} \delta_{ij} \delta_{ik} \lambda_i \lambda_j \log(\lambda_k^2) \tag{C.7}$$

$$= -\sum_{k} p_k \log p_k \tag{C.8}$$

where we have set $\lambda_k^2 = p_k$ because each Schmidt coefficient is real. δ_{ij} are Kronecker deltas because we have chosen the basis $\{|s_k\rangle\}$ to be orthonormal. Note that $\sum_k p_k = 1$. In this

case, the second term is nothing but S(A) = S(B) which is the von Neumann entropy of a subsystem.

Since we have chosen a particular stabilizer state σ_{AB} , this serves as an upper bound of the relative entropy of magic. Hence

$$M_R^{(NL)}(\rho_{AB}) \le M_R^{(NL)}(\psi_{AB}) \le S(A) = S(B).$$
 (C.9)

C.3 Proof of Theorem 4

Let ρ_{AB}^{ϵ} represent the state that minimizes the non-local magic. Therefore $M_{RS}^{(NL,\epsilon)}(\rho_{AB}) = M_{RS}^{(NL)}(\rho_{AB}^{\epsilon})$. Drawing from Theorem 2, we understand that:

$$M_{RS}^{(NL,\epsilon)}(\rho_{AB}) \ge S_{max}(\rho_A^{\epsilon}) - S(\rho_A^{\epsilon}) \ge \min_{\|\chi - \rho_A\| < \epsilon} (S_{max}(\chi) - S(\chi)). \tag{C.10}$$

On the right-hand side, our goal is to identify a state χ within the ϵ -ball of ρ_A that minimizes the difference between $S_{max}(\chi)$ and $S(\chi)$. Interestingly, the state that minimizes this difference also reduces $S_{max}(\chi)$ to its lowest value S_{max}^{ϵ} . To illustrate, denote χ_A^{ϵ} as the state that minimizes S_{max} within the ϵ -ball. Then consider increasing S_{max} by modifying one eigenvalue of χ_A^{ϵ} from zero to δ . This adjustment results in an increase $\Delta S_{max} = e^{-S_{max}}$, while the change in entropy is capped at $\Delta S \leq \delta |\log \delta|$. Such a modification invariably elevates the entropy gap, i.e. $\Delta(S_{max} - S) \geq e^{-S_{max}} - \delta |\log \delta| > 0$, since δ can be arbitrarily small.

To evaluate the von Neumann entropy of the state χ_A^{ϵ} , as a modification from ρ_A by dropping some eigenvalues whose total contribution to the trace is smaller than ϵ . Let's denote their contribution to the von Neumann entropy as S_{ϵ} . Then the entropy of the new state χ_A^{ϵ} is given by $S(\chi_A^{\epsilon}) = \frac{S(\rho_A) - S_{\epsilon}}{1 - \epsilon} \leq \frac{S(\rho_A)}{1 - \epsilon}$. Therefore, we get the following inequality:

$$M_{RS}^{(NL,\epsilon)}(\rho_{AB}) \ge S_{max}(\chi_A^{\epsilon}) - S(\chi_A^{\epsilon})$$

$$\ge S_{max}^{\epsilon}(\rho_A) - (1 - \epsilon)^{-1}S(\rho_A). \tag{C.11}$$

Regarding the upper bound, since χ_A^{ϵ} minimizes the maximal entropy, it satisfies the following condition:

$$S_{max}^{\epsilon}(\rho_A) = S_{max}(\chi_A^{\epsilon}). \tag{C.12}$$

While this condition specifies the spectrum of χ_A^{ϵ} , we retain the flexibility to select a purification χ_{AB}^{ϵ} , ensuring its deviation from ρ_{AB} remains within an ϵ bound. Consequently, the process of minimizing the non-local magic leads us to the following inequality:

$$\begin{split} M_{RS}^{(NL,\epsilon)}(\rho_{AB}) \leq & M_{RS}^{(NL)}(\chi_{AB}^{\epsilon}) \\ \leq & (\log d) \lceil \log_d \operatorname{rank} \chi_{AB}^{\epsilon} \rceil = \log d \lceil S_{max}^{\epsilon}(A) / \log d \rceil. \end{split} \tag{C.13}$$

where the second step is a result from Theorem 2.

D Estimate by Stabilizer-Rényi-entropy

D.1 Proof of Theorem 3

In this section, we provide an estimation of the second Stabilizer-Rényi-entropy measure of the non-local magic. It is defined in [42] as the second Rényi-entropy of a probability distribution, $p_a = \frac{1}{d} |\langle \psi | P_a | \psi \rangle|^2$, over all the Pauli-string basis P_a .

$$\mathcal{M}_2(|\psi\rangle) := -\log(\sum_a p_a^2) - \log d. \tag{D.1}$$

Given the entanglement spectrum $\{\lambda_i\}$, we construct a state $|\psi'\rangle$ with small local magic,

$$|\psi'\rangle_{AB} = \sum_{i=0}^{r-1} \sqrt{\lambda_i} |s_i\rangle_A |s_i\rangle_B.$$
 (D.2)

where the rank r is taken to be 2^n for integer n. The Pauli operators on the Hilbert space $\mathcal{H}_{AB} = \mathcal{H}_A \otimes \mathcal{H}_B$ can be factorized as product of Pauli operators on \mathcal{H}_A and \mathcal{H}_B respectively, $P^{ab} = P^a \otimes P^b$. We denote their matrix elements as $P_{ij}^{a,b} := \langle s_i | P^{a,b} | s_j \rangle$, and compute the magic measure \mathcal{M}_2 as follows,

$$\mathcal{M}_2(|\psi'\rangle) = -\log\left(\sum_{a=1}^{r^2} \sum_{b=1}^{r^2} \left| \sum_{i,j=0}^{r-1} \sqrt{\lambda_i} \sqrt{\lambda_j} P_{ij}^a P_{ij}^b \right|^4\right). \tag{D.3}$$

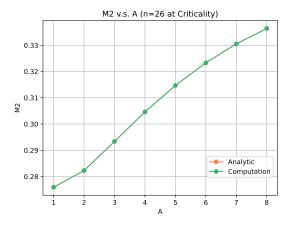
The result is complicated and depends on specific choice of the basis $|s_i\rangle$'s. We simplify the analysis by assuming that the orthonormal basis $|s_i\rangle$'s are common eigenstates of a stabilizer group $\mathcal{S} = \{S_1, S_2, \dots, S_n\}$. This condition allows us to write the Pauli matrices P_{ij}^a in computational basis. Substituting the matrix representation of Pauli operators, we find that

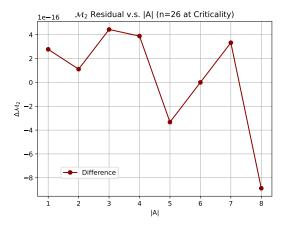
$$\mathcal{M}_{2} = -\log\left(\sqrt{\lambda_{i_{1}}}\sqrt{\lambda_{i_{2}}}\sqrt{\lambda_{i_{3}}}\sqrt{\lambda_{i_{4}}}\sqrt{\lambda_{i_{5}}}\sqrt{\lambda_{i_{6}}}\sqrt{\lambda_{i_{7}}}\sqrt{\lambda_{i_{8}}}\left(\sum_{a}P_{i_{1}i_{2}}^{a}P_{i_{3}i_{4}}^{a}P_{i_{5}i_{6}}^{a}P_{i_{7}i_{8}}^{a}\right)^{2}\right)$$

$$= -\log\left(\sum_{i_{1},i_{2},i_{3},i_{4}=0}^{r-1}\sqrt{\lambda_{i_{1}}\lambda_{i_{2}}\lambda_{i_{3}}\lambda_{i_{4}}\lambda_{i_{3}\wedge i_{2}\wedge i_{1}}\lambda_{i_{4}\wedge i_{2}\wedge i_{1}}\lambda_{i_{1}\wedge i_{3}\wedge i_{4}}\lambda_{i_{2}\wedge i_{3}\wedge i_{4}}}\right).$$
(D.4)

where \land denotes the bitwise XOR operation. This expression depends on order of eigenvalues and takes minimum when the eigenvalues are ordered, $\lambda_i > \lambda_j$ for i < j. If we take all the eigenvalues to be the same, then each term in the summation is equal to $\frac{1}{r^4}$. The number of terms is r^4 since we are summing over four indices. The argument is equal to 1 in this case. Therefore, the non-local Stabilizer Rényi entropy vanishes when the spectrum is flat.

Fig. 12 gives a comparison of the direct SRE calculation against the estimation given by Eq. (D.4). As can be observed in the plots, the approximation in Eq. (D.4) is correct up to numerical imprecision.





- (a) \mathcal{M}_2 computed from stabilizer Rényi entropy, compared to the estimation in Eq. (D.4).
- (b) Residual from computational and analytic calculations of \mathcal{M}_2 , accurate to one part in 10^{16} .

Figure 12

We can derive an upper bound for \mathcal{M}_2 , by averaging over the permutations of eigenvalues, this gives us the expression,

$$\mathcal{M}_{2} \leq \overline{\mathcal{M}}_{2} = -\log \left(\sum_{i=0}^{r-1} \lambda_{i}^{4} + 7 \sum_{0 \leq i \neq j \leq r-1} \lambda_{i}^{2} \lambda_{j}^{2} + \frac{7}{r-3} \sum_{0 \leq i \neq j \neq k \neq l \leq r-1} \lambda_{i} \lambda_{j} \lambda_{k} \lambda_{l} + \frac{\sum_{0 \leq i_{1} \neq i_{2} \neq \cdots \neq i_{8} \leq r-1} \prod_{a=1}^{8} \sqrt{\lambda_{i_{a}}}}{(r-3)(r-5)(r-6)(r-7)} \right).$$
(D.5)

In Eq. (D.5), the sum inside the logarithm is taken over products of distinct eigenvalues. Computing this sum explicitly, and expressing the result in terms of different Rényi entropies S_{α} , we obtain

$$\overline{\mathcal{M}}_{2} = -\log\left(7e^{-2S_{2}} - 6e^{-3S_{4}} + 7e^{-S_{0}}(1 - 6e^{-S_{2}} + 8e^{-2S_{3}} + 3e^{-2S_{2}}) + e^{-4S_{0}}(e^{4S_{1/2}} + 105e^{-3S_{4}} - 420e^{S_{1/2}} + \cdots)\right)$$

$$= -\log\left(7e^{-2S_{2}} - 6e^{-3S_{4}} + e^{4S_{1/2} - 4S_{0}}\right) + O(e^{-S_{1/2}}).$$
(D.6)

The averaged magic $\overline{\mathcal{M}}_2$ is a complicated combination of Rényi entropies, ranging from $S_{1/2}$ to S_4 . However, in the large Hilbert dimension limit, where $S_{1/2} \gg 1$, the averaged magic $\overline{\mathcal{M}}_2$ simplifies to the final expression in Eq. (D.6). It provides a straightforward estimate of \mathcal{M}_2 based on a few Rényi entropy terms.

To establish a rigorous bound for \mathcal{M}_2 , we start with Eq. (D.5), leading to:

$$\overline{\mathcal{M}}_{2} \leq -\log \left(\sum_{i=0}^{r-1} \lambda_{i}^{4} + 7 \sum_{0 \leq i \neq j \leq r-1} \lambda_{i}^{2} \lambda_{j}^{2} \right)$$

$$\leq -\log \left(\left(\sum_{i} \lambda_{i}^{2} \right)^{2} \right) = 2S_{2}.$$
(D.7)

This holds for all spectrum distributions. Rewriting Eq. (D.5) in terms of the entropy difference $\delta_{1/2} = S_0 - S_{1/2}$, we obtain the following expansion;

$$\overline{\mathcal{M}}_2 = -\log\left(e^{-4\delta_{1/2}} + e^{-S_0}(7 + 21e^{-4\delta_{1/2}} - 28e^{-3\delta_{1/2}}) + O(e^{-2S_0})\right)$$

$$\leq 4\delta_{1/2}.$$
(D.8)

Note that the coefficient associated with e^{-S_0} in the expansion remains non-negative for any value of $\delta_{1/2}$ and vanishes when $\delta_{1/2} = 0$. Verifying that these coefficients are non-negative for every order of e^{-S_0} supports the inequality. Finally, combining this with the previously established bound finishes our proof that:

$$\mathcal{M}_2(\{\lambda_i\}) \le \overline{\mathcal{M}}_2 \le \min\{2S_2, 4(S_0 - S_{1/2})\}.$$
 (D.9)

D.2 Proof of Proposition 8

Let $|\phi\rangle$ denotes an entangled pair of qubits, with the entanglement spectrum given by $\{\lambda, 1 - \lambda\}$. We show that the non-local stabilizer Rényi entropy $\mathcal{M}_2(\lambda)$ of $|\phi\rangle$ is bounded by the non-flatness $\partial_n \tilde{S}_n$.

From Eq. (3.53), we find that $\mathcal{M}_2(\lambda)$ is equal to,

$$\mathcal{M}_2(\lambda) = -\log(1 - 4\lambda + 20\lambda^2 - 32\lambda^3 + 16\lambda^4).$$
 (D.10)

By definition Eq. (3.26), the non-flatness is

$$-\partial_n \tilde{S}_n = n \frac{\lambda^n (1-\lambda)^n \left(\log \frac{\lambda}{1-\lambda}\right)^2}{\left(\lambda^n + (1-\lambda)^n\right)^2}.$$
 (D.11)

Both functions are zero at $\lambda = 0$, $\frac{1}{2}$, 1. So let's make a Taylor expansion around these value. Around $\lambda = \frac{1}{2}$, we have that

$$\mathcal{M}_{2}(\lambda) = 4(\lambda - 1/2)^{2} - 8(\lambda - 1/2)^{4} + O((\lambda - 1/2)^{5})$$

$$-\partial_{n}\tilde{S}_{n}|_{n=1} = 4(\lambda - 1/2)^{2} - \frac{16}{3}(\lambda - 1/2)^{4} + O((\lambda - 1/2)^{5})$$

$$-\frac{1}{2}\partial_{n}\tilde{S}_{n}|_{n=2} = 4(\lambda - 1/2)^{2} - \frac{160}{3}(\lambda - 1/2)^{4} + O((\lambda - 1/2)^{5}).$$
(D.12)

Therefore for λ close to 1/2, the following inequality holds:

$$-\frac{1}{2}\partial_n \tilde{S}_n|_{n=2} \le \mathcal{M}_2(\lambda) \le -\partial_n \tilde{S}_n|_{n=1}. \tag{D.13}$$

Similarly, one can show that this inequality holds for λ close to 0 and 1, where the functions are,

$$\mathcal{M}_{2}(\lambda) = 4\lambda - 12\lambda^{2} + O(\lambda^{3})$$

$$-\partial_{n}\tilde{S}_{n}|_{n=1} = \lambda \log^{2} \lambda + (2\log \lambda - \log^{2} \lambda)\lambda^{2} + O(\lambda^{3})$$

$$-\frac{1}{2}\partial_{n}\tilde{S}_{n}|_{n=2} = \lambda^{2} \log^{2} \lambda + 2(\log \lambda + \log^{2} \lambda)\lambda^{3} + O(\lambda^{4}).$$
(D.14)

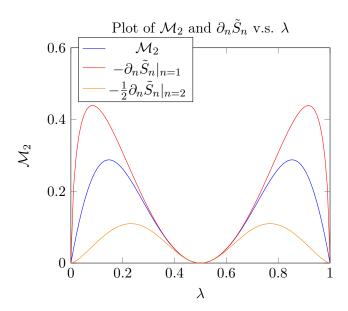


Figure 13: The non-local stabilizer Rényi entropy \mathcal{M}_2 is bounded by the anti-flatness $\partial_n \tilde{S}_n$

For other value of λ , we justify this inequality by the plot in Fig. 13.

Both the Stabilizer Rényi entropy and anti-flatness are additive. Therefore for state $|\psi\rangle$ that can be distilled into product of entangled pairs $U_A \otimes U_B |\psi\rangle_{AB} = \bigotimes_{i=1}^k |\phi\rangle_{a_ib_i}$, we have,

$$\frac{1}{2} \left| \frac{\partial_n \mathcal{A}_n|_{n=2}}{4G} (|\psi\rangle_{AB}) \right| \le \mathcal{M}_2(|\psi\rangle_{AB}) \le \left| \frac{\partial_n \mathcal{A}_n|_{n=1}}{4G} (|\psi\rangle_{AB}) \right|. \tag{D.15}$$

D.3 Distillation of Matrix Product State

We further elaborate our discussions from Section 4.1. Building on the MERA representation of CFT, we transform the state on the boundary of the past light-cone, ∂A , into a Matrix Product State (MPS) using local unitaries, as defined in Eq. (4.1) and illustrated in Fig. 2. In this section, we further contend that this MPS state can approximately be distilled into a tensor product of entangled pairs:

$$|\chi\rangle_{AB} \approx U_A \otimes U_B \left(\bigotimes_{i=1}^k |\phi_i\rangle_{a_i b_i} \right).$$
 (D.16)

where k is the size of MPS state. It's clear that this approximation does not hold in general due to the disparity in the number of free parameters between the most general entanglement spectrum (contains 2^{k-1} parameters) and that of the tensor product of entangled pairs (k parameters). However, for translationally invariant MPS states characterized by short correlation lengths, this approximation is valid.

To substantiate this approximation, we simulate several MPS states using k number of identical random matrices to construct the reduced state $\rho_A = \operatorname{tr}_B(|\chi\rangle\langle\chi|)$ and evaluate its entanglement spectrum. We then approximate this spectrum by fitting it to the tensor

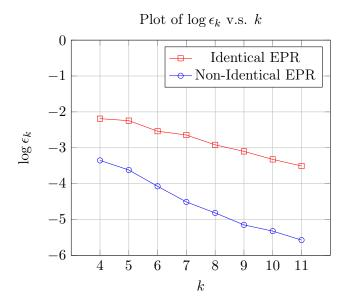


Figure 14: Scaling of error with system size.

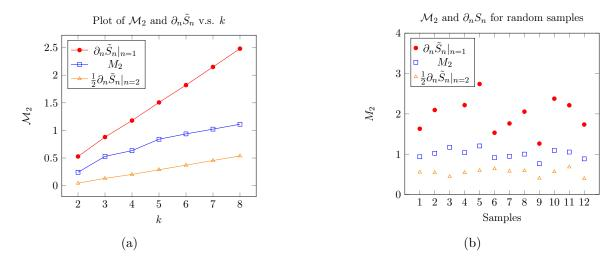


Figure 15: (a) Scaling of \mathcal{M}_2 and $\partial_n \tilde{S}_n$ with state size k for a particular sample of random matrix in MPS. (b) For randomly generated samples of MPS states with a fixed size k = 7, \mathcal{M}_2 is bounded by anti-flatness $\partial_n \tilde{S}_n$.

product of individual entangled pair spectra:

$$\min_{\{\lambda_i\}} \left| \operatorname{Spec}(\rho_A) - \bigotimes_{i=1}^k \begin{pmatrix} \lambda_i & 0\\ 0 & 1 - \lambda_i \end{pmatrix} \right| = \epsilon_k \tag{D.17}$$

where ϵ_k quantifies the approximation error. Our numerical analysis up to k = 11 reveals an exponential decrease in ϵ_k with increasing k. We present two distinct scenarios in Fig. 14: In the first scenario, we require all EPR pairs in the tensor product to be identical, yielding an error trend of $\epsilon_k \sim 0.1 \times 1.2^{-k}$. In the second scenario, we relax this constraint, allowing

for variability among the EPR pairs, which results in a more pronounced error reduction, following $\epsilon_k \sim 0.05 \times 1.4^{-k}$.

With the distillation assumption justified we expect the inequality Eq. (D.15) to be true for general MPS state and therefore for a CFT. We plot the magic and the Rényi entropy (dual to brane area) for a set of randomly generated samples of MPS states in Fig. 15 and verify the validity of the bound Eq. (D.15).

E Validity of various bound for magic

In the main text, we introduced several approximations for non-local magic, noting its proportional relationship to anti-flatness in certain regimes and its closeness to entropy in others. This section delineates the conditions under which these approximations hold true.

Near flat limit

We begin by examining the approximation between non-local magic and anti-flatness, specifically:

$$\mathcal{M}_2(|\psi\rangle_{AB}) \approx \frac{\mathcal{F}(\rho_A)}{\text{Pur}^2(\rho_A)},$$
 (E.1)

which is applicable primarily in the near-flat limit of the entanglement spectrum. This is because the left-hand side (LHS) is additive and scales linearly with n, while the right-hand side (RHS) can be expressed as:

$$\frac{\mathcal{F}(\rho_A)}{\operatorname{Pur}^2(\rho_A)} = \frac{\operatorname{tr}(\rho_A^3) - \operatorname{tr}(\rho_A^2)^2}{\operatorname{tr}(\rho_A^2)^2} = e^{2(S_2(A) - S_3(A))} - 1,$$
 (E.2)

which becomes additive only at the linear order of the Taylor expansion in the entropy difference. Hence, the condition $S_2(A) - S_3(A) < \frac{1}{2}$ must be met, indicating an almost flat spectrum or a small system size.

Additionally, this regime aligns with where the two anti-flatness measures defined previously converge, particularly when:

$$\langle (\delta \log \rho)^2 \rangle_{\rho} \approx \frac{\langle (\delta \rho)^2 \rangle_{\rho}}{\langle \rho \rangle_{\rho}^2}$$
 (E.3)

under the condition $\sum_i \delta \lambda_i^2 \ll \sum_i \bar{\lambda}_i^2$. In the flat limit $\sum_i \bar{\lambda}_i^2 \sim e^{-S_0}$. and $\sum_i \delta \lambda_i^2 \sim e^{-S_2} - e^{-S_0}$. So the approximation requires $e^{S_0 - S_2} - 1 < 1$, that is $S_0 - S_2 \sim O(1)$. This also corresponds to near-flat regime or small system size.

Far from flat limit

In contrast, for quantum states with a far-from-flat entanglement spectrum, where the entropy differences across Rényi indices are comparable to the entropy itself, the scenario changes. Referring to Theorem 3, the upper bound for the second Stabilizer Rényi entropy measure of non-local magic is:

$$\mathcal{M}_2^{NL}(|\psi\rangle_{AB}) \le \mathcal{M}_2(\{\lambda_i\}) \le \min\{2S_2(A), 4(S_0(A) - S_{1/2}(A))\},$$
 (E.4)

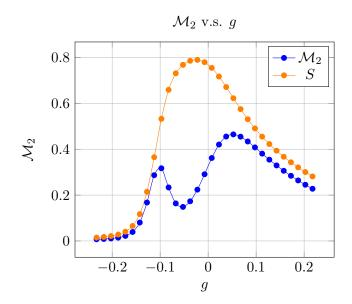


Figure 16: Plot of \mathcal{M}_2 v.s. g, at $b = 10^{-4}$ and |A| = 9.

indicating a transitional crossover around $S_0(A) - S_{1/2}(A) \sim \frac{1}{2}S_2(A)$. Beyond this point, non-local magic transitions from being proportional to anti-flatness to being proportional to entropy. Our numerical analyses within the Ising model confirm this transition: in the disordered phase and at critical points, non-local magic correlates with entropy S both when varying the model parameter and the subsystem size. However, in the symmetry-breaking phase (refer to Appendix F.1), it deviates and becomes anti-correlated with entropy, as shown in Fig. (17).

F Supplemental results for Ising Model

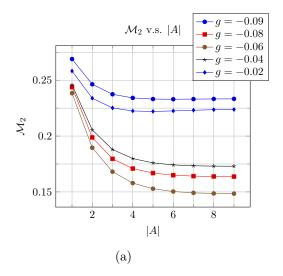
F.1 Symmetry breaking phase

In the g < 0 regime, the Ising model enters the symmetry-breaking phase in the thermodynamic limit. However, our analysis is conducted on a finite-size lattice, where the ground state remains symmetric to spin flipping. Heuristically, we can think of this ground state being approximated by something similar to the GHZ state:

$$|G\rangle_{sym} \approx \frac{1}{\sqrt{2}}(|00\cdots 0\rangle + |11\cdots 1\rangle).$$
 (F.1)

To approximate the true ground state achievable in the thermodynamic limit within our finite lattice model, we introduce a small bias field in the z-direction:

$$H = H_{\text{Ising}}(g) + b \sum_{i} Z_{i}. \tag{F.2}$$



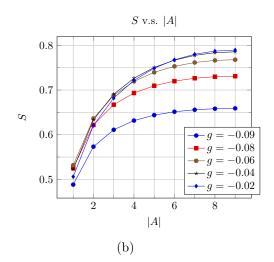


Figure 17: (a)Non-local magic \mathcal{M}_2 v.s. |A|. (b) Entropy S v.s. |A|, at $b = 10^{-5}$ and g > -0.1.

As the bias b increases, the ground state transitions towards one of the two symmetry-broken states:

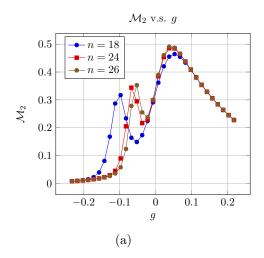
$$|G\rangle_{\uparrow} = |\uparrow\uparrow\cdots\uparrow\rangle \tag{F.3}$$

$$|G\rangle_{\downarrow} = |\downarrow\downarrow\cdots\downarrow\rangle. \tag{F.4}$$

Exploring how non-local magic \mathcal{M}_2 behaves as we adjust different parameters led to some fascinating results that are particularly noticeable when a non-zero bias field is applied. As shown in Fig. 16, a distinctive "valley" emerges in the \mathcal{M}_2 plot within the g < 0 regime. We juxtapose entropy and non-local magic in our plots to underscore their divergent behaviors and the unique information conveyed by non-local magic.

This valley can be understood as arising from the competition between two types of ground states. Within the valley, the system's ground state approximates the symmetric GHZ-like state $|G\rangle_{sym}$, as defined in Eq. (F.1). In this region, non-local magic values are minimized because the reduced density matrix of $|G\rangle_{sym}$ resembles that of a maximally mixed single qubit state, leading to a flat spectrum and, consequently, lower \mathcal{M}_2 follows from Corollary 3.1. Additionally, we observe diminished \mathcal{M}_2 values in regions far from the critical point, where |g| is sufficiently large, as indicated by the plateau beyond g < -0.2 in Fig. 16. Here, the ground state transitions to a symmetry-broken state $|G\rangle_{\uparrow/\downarrow}$, which lacks non-local magic due to its tensor product structure.

Despite the low non-local magic values associated with both $|G\rangle_{sym}$ and $|G\rangle_{\uparrow/\downarrow}$, the transition between these states has to past through a regime of non-trivial non-local magic. This occurs because continuous parameter changes cannot be approximated by discrete Clifford transformations, resulting in a notable increase in non-local magic. The \mathcal{M}_2 measure captures this as a pronounced peak, delineating the transition between the two ground states near $g \sim -0.1$ in Fig. 16.



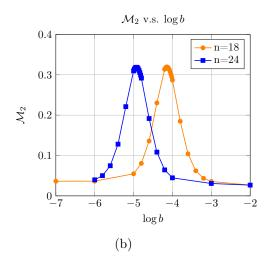


Figure 18: (a) Plot of \mathcal{M}_2 v.s. g, at $b = 10^{-4}$. The lattice size takes n = 18, n = 24 and n = 26; (b) Plot of \mathcal{M}_2 v.s. $\log b$, at g = -0.11, with lattice size taking n = 18 and n = 24

An additional noteworthy aspect of non-local magic inside the valley is its counterintuitive decrease with increasing subregion size |A|, as depicted in Fig. 17a. This phenomenon is unique to the valley. In contrast, entropy consistently increases with |A|. This unusual trend in \mathcal{M}_2 is also linked to the proximity to the symmetric state $|G\rangle_{sym}$, which results in an almost flat entanglement spectrum within the valley. Consequently, \mathcal{M}_2 aligns more closely with the entropy differential $S_0 - S$ rather than the entropy itself, as discussed in Section 3.3.3, offering an explanation for the inverse relationship observed between S and \mathcal{M}_2 in this region.

It's also important to note that the competition between $|G\rangle_{sym}$ and $|G\rangle_{\uparrow/\downarrow}$ is a manifestation of finite-size effects. As demonstrated in Fig. 18, the valley tends to diminish with increasing lattice size n. Specifically, when we set $b=10^{-4}$ (see Fig. 18a), the peak of non-local magic shifts closer to g=0 with larger lattice sizes. Similarly, with g=-0.11 (see Fig. 18b), the peak moves towards b=0 as the lattice size expands. This suggests that the parameter space favoring the symmetric state narrows in both dimensions with increasing lattice size.

Expanding our analysis, Fig. 19 explores the non-local magic across a broader range of the bias field b. We find that beyond b > 0.01 the valley disappears, and the g < 0 phase transitions to being governed by the symmetry-broken ground state $|G\rangle_{\uparrow/\downarrow}$. As b decreases towards zero, the peak is pushed to the left where the valley widens, signifying the growing significance of the symmetric ground state $|G\rangle_{sym}$, which becomes dominant for all g < 0 in the absence of b.

Fig. (20) depicts the \mathcal{M}_2 surface as a function of subregion size |A| and critical angle θ . As we decrease the magnitude of the bias field, the symmetry-breaking peak is pushed towards lower and lower θ values.

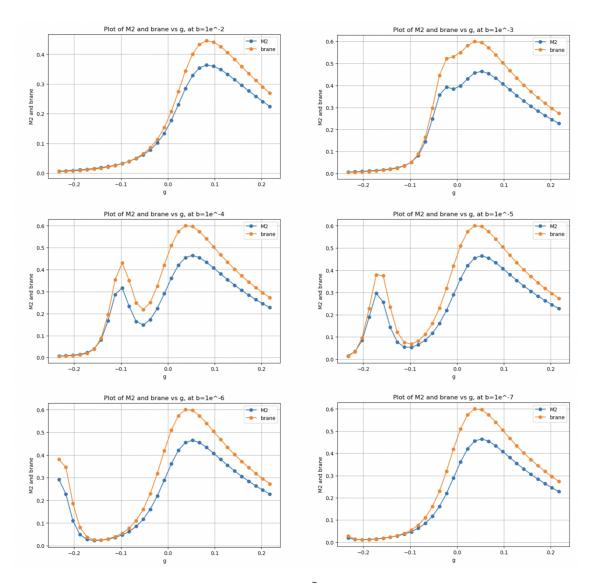
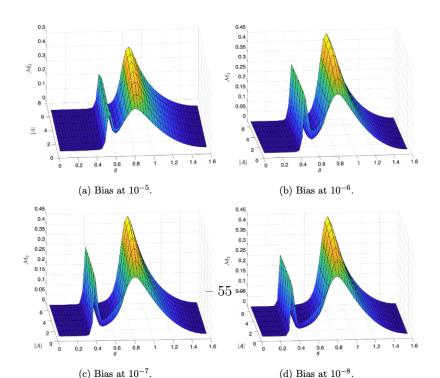


Figure 19: Comparison between \mathcal{M}_2 and $|\partial_n \tilde{S}_n|$ (labeled as brane) at various magnetic field b and model parameter g. The small peak separates and is pushed to the left as b decreases.



References

- [1] A. Kitaev and J. Preskill, *Topological Entanglement Entropy*, Physical Review Letters **96**, 110404 (2006), doi:10.1103/PhysRevLett.96.110404.
- [2] M. Levin and X.-G. Wen, *Detecting Topological Order in a Ground State Wave Function*, Physical Review Letters **96**, 110405 (2006), doi:10.1103/PhysRevLett.96.110405.
- [3] A. Hamma, R. Ionicioiu and P. Zanardi, Bipartite entanglement and entropic boundary law in lattice spin systems, Physical Review A 71, 022315 (2005), doi:10.1103/PhysRevA.71.022315.
- [4] P. Hosur, X.-L. Qi et al., Chaos in quantum channels, Journal of High Energy Physics **2016**(2), 4 (2016), doi:10.1007/JHEP02(2016)004.
- [5] C. W. von Keyserlingk, T. Rakovszky et al., Operator Hydrodynamics, OTOCs, and Entanglement Growth in Systems without Conservation Laws, Physical Review X 8, 021013 (2018), doi:10.1103/PhysRevX.8.021013.
- [6] A. Nahum, S. Vijay and J. Haah, Operator Spreading in Random Unitary Circuits, Physical Review X 8, 021014 (2018), doi:10.1103/PhysRevX.8.021014.
- [7] B. Skinner, J. Ruhman and A. Nahum, Measurement-Induced Phase Transitions in the Dynamics of Entanglement, Physical Review X 9, 031009 (2019), doi:10.1103/PhysRevX.9.031009.
- [8] M. Van Raamsdonk, Building up spacetime with quantum entanglement, Gen. Rel. Grav.
 42, 2323 (2010), doi:10.1142/S0218271810018529, 1005.3035.
- [9] A. Almheiri, D. Marolf et al., Black holes: complementarity or firewalls?, Journal of High Energy Physics **2013**(2) (2013), doi:10.1007/jhep02(2013)062.
- [10] J. Maldacena and L. Susskind, Cool horizons for entangled black holes, Fortschritte der Physik 61(9), 781–811 (2013), doi:10.1002/prop.201300020.
- [11] J. Maldacena, International Journal of Theoretical Physics 38(4), 1113–1133 (1999), doi:10.1023/a:1026654312961.
- [12] E. Witten, Anti-de Sitter space and holography, Adv. Theor. Math. Phys. 2, 253 (1998), doi:10.4310/ATMP.1998.v2.n2.a2, hep-th/9802150.
- [13] B. Czech and L. Lamprou, *Holographic definition of points and distances*, Phys.Rev. D **90**(10), 106005 (2014), doi:10.1103/PhysRevD.90.106005.
- [14] B. Czech, X. Dong and J. Sully, Holographic reconstruction of general bulk surfaces, Journal of High Energy Physics 2014(11) (2014), doi:10.1007/jhep11(2014)015.
- [15] B. Czech, L. Lamprou et al., Equivalent equations of motion for gravity and entropy, Journal of High Energy Physics **2017**(2) (2017), doi:10.1007/jhep02(2017)004.
- [16] C. Cao, X.-L. Qi et al., Building bulk geometry from the tensor radon transform, Journal of High Energy Physics **2020**(12) (2020), doi:10.1007/jhep12(2020)033.
- [17] N. Bao, C. Cao et al., Towards Bulk Metric Reconstruction from Extremal Area Variations, Class. Quant. Grav. 36(18), 185002 (2019), doi:10.1088/1361-6382/ab377f, 1904.04834.
- [18] S. Ryu and T. Takayanagi, Holographic derivation of entanglement entropy from the anti-de sitter space/conformal field theory correspondence, Physical Review Letters **96**(18) (2006), doi:10.1103/physrevlett.96.181602.

- [19] A. Lewkowycz and J. Maldacena, Generalized gravitational entropy, Journal of High Energy Physics 2013(8) (2013), doi:10.1007/jhep08(2013)090.
- [20] T. Faulkner, A. Lewkowycz and J. Maldacena, Quantum corrections to holographic entanglement entropy, Journal of High Energy Physics 2013(11) (2013), doi:10.1007/jhep11(2013)074.
- [21] V. E. Hubeny, M. Rangamani and T. Takayanagi, A covariant holographic entanglement entropy proposal, Journal of High Energy Physics 2007(07), 062–062 (2007), doi:10.1088/1126-6708/2007/07/062.
- [22] D. Harlow, The Ryu-Takayanagi Formula from Quantum Error Correction, Communications in Mathematical Physics 354(3), 865 (2017), doi:10.1007/s00220-017-2904-z, 1607.03901.
- [23] F. Pastawski, B. Yoshida et al., Holographic quantum error-correcting codes: toy models for the bulk/boundary correspondence, Journal of High Energy Physics 2015(6) (2015), doi:10.1007/jhep06(2015)149.
- [24] P. Hayden, S. Nezami *et al.*, *Holographic duality from random tensor networks*, Journal of High Energy Physics **2016**(11) (2016), doi:10.1007/jhep11(2016)009.
- [25] Z. Yang, P. Hayden and X.-L. Qi, Bidirectional holographic codes and sub-ads locality, Journal of High Energy Physics **2016**(1) (2016), doi:10.1007/jhep01(2016)175.
- [26] R. J. Harris, N. A. McMahon et al., Calderbank-shor-steane holographic quantum error-correcting codes, Physical Review A 98(5) (2018), doi:10.1103/physreva.98.052301.
- [27] C. Cao and B. Lackey, Approximate bacon-shor code and holography, Journal of High Energy Physics **2021**(5) (2021), doi:10.1007/jhep05(2021)127.
- [28] M. Steinberg, S. Feld and A. Jahn, *Holographic codes from hyperinvariant tensor networks*, Nature Communications **14**(1) (2023), doi:10.1038/s41467-023-42743-z.
- [29] T. Jacobson, Entanglement equilibrium and the einstein equation, Physical Review Letters 116(20) (2016), doi:10.1103/physrevlett.116.201101.
- [30] C. Cao, S. M. Carroll and S. Michalakis, Space from hilbert space: Recovering geometry from bulk entanglement, Physical Review D 95(2) (2017), doi:10.1103/physrevd.95.024031.
- [31] C. Cao and S. M. Carroll, Bulk entanglement gravity without a boundary: Towards finding einstein's equation in hilbert space, Physical Review D 97(8) (2018), doi:10.1103/physrevd.97.086003.
- [32] X. Dong, S. McBride and W. W. Weng, Holographic tensor networks with bulk gauge symmetries, arXiv (2023), [hep-th/2309.06436].
- [33] C. Akers and A. Y. Wei, Background independent tensor networks, arXiv (2024), [hep-th/2402.05910].
- [34] N. Cheng, C. Lancien et al., Random tensor networks with nontrivial links, arXiv (2022), [quant-ph/2206.10482].
- [35] C. Cao, J. Pollack and Y. Wang, Hyperinvariant multiscale entanglement renormalization ansatz: Approximate holographic error correction codes with power-law correlations, Phys. Rev. D 105, 026018 (2022), doi:10.1103/PhysRevD.105.026018.
- [36] N. Bao, G. Penington et al., Beyond toy models: Distilling tensor networks in full ads/cft, JHEP **2019**(11), 69 (2019), doi:10.1007/JHEP11(2019)069, 1812.01171.

- [37] C. Akers and P. Rath, Entanglement Wedge Cross Sections Require Tripartite Entanglement, JHEP 04, 208 (2020), doi:10.1007/JHEP04(2020)208, 1911.07852.
- [38] P. Hayden, O. Parrikar and J. Sorce, The Markov gap for geometric reflected entropy, JHEP 10, 047 (2021), doi:10.1007/JHEP10(2021)047, 2107.00009.
- [39] C. Cao, Stabilizer codes have trivial area operators, arXiv (2023), [hep-th/2306.14996].
- [40] S. Bravyi and A. Kitaev, Universal quantum computation with ideal Clifford gates and noisy ancillas, Physical Review A 71, 022316 (2005), doi:10.1103/PhysRevA.71.022316.
- [41] V. Veitch, S. A. H. Mousavian et al., The resource theory of stabilizer quantum computation, New Journal of Physics 16(1), 013009 (2014), doi:10.1088/1367-2630/16/1/013009.
- [42] L. Leone, S. F. E. Oliviero and A. Hamma, Stabilizer Rényi Entropy, Phys. Rev. Lett. 128(5), 050402 (2022), doi:10.1103/PhysRevLett.128.050402, 2106.12587.
- [43] K. Bu, W. Gu and A. Jaffe, Stabilizer Testing and Magic Entropy, arxiv, doi:10.48550/arXiv.2306.09292 (2023), [math-ph, physics:quant-ph/2306.09292].
- [44] C. D. White, C. Cao and B. Swingle, *Conformal field theories are magical*, Physical Review B **103**, 075145 (2021), doi:10.1103/PhysRevB.103.075145.
- [45] S. Sarkar, C. Mukhopadhyay and A. Bayat, Characterization of an operational quantum resource in a critical many-body system, New Journal of Physics 22(8), 083077 (2020), doi:10.1088/1367-2630/aba919.
- [46] Z.-W. Liu and A. Winter, Many-Body Quantum Magic, PRX Quantum 3, 020333 (2022), doi:10.1103/PRXQuantum.3.020333.
- [47] P. S. Tarabunga, E. Tirrito et al., Many-body magic via Pauli-Markov chains from criticality to gauge theories, PRX Quantum 4(4), 2305.18541 (2023), doi:10.1103/PRXQuantum.4.040317, 2305.18541.
- [48] K. Goto, T. Nosaka and M. Nozaki, Probing chaos by magic monotones, Phys. Rev. D 106, 126009 (2022), doi:10.1103/PhysRevD.106.126009.
- [49] T. J. Sewell and C. D. White, Mana and thermalization: Probing the feasibility of near-Clifford Hamiltonian simulation (2022), doi:10.48550/ARXIV.2201.12367.
- [50] D. Rattacaso, L. Leone et al., Stabilizer entropy dynamics after a quantum quench, arxiv, doi:10.48550/arXiv.2304.13768 (2023), [quant-ph/2304.13768].
- [51] L. Leone, S. F. E. Oliviero et al., Phase transition in stabilizer entropy and efficient purity estimation, Phys. Rev. A 109, 032403 (2024), doi:10.1103/PhysRevA.109.032403.
- [52] P. Niroula, C. D. White et al., Phase transition in magic with random quantum circuits (2023), 2304.10481.
- [53] L. Leone, S. F. E. Oliviero et al., Quantum Chaos is Quantum, Quantum 5, 453 (2021), doi:10.22331/q-2021-05-04-453.
- [54] S. F. E. Oliviero, L. Leone and A. Hamma, Transitions in entanglement complexity in random quantum circuits by measurements, Physics Letters A 418, 127721 (2021), doi:10.1016/j.physleta.2021.127721.
- [55] M. Bejan, C. McLauchlan and B. Béri, Dynamical magic transitions in monitored clifford+t circuits, arXiv (2023), [quant-ph/2312.00132].

- [56] C. Vairogs and B. Yan, Extracting randomness from quantum 'magic', arXiv (2024), [quant-ph/2402.10181].
- [57] S. F. E. Oliviero, L. Leone and A. Hamma, Magic-state resource theory for the ground state of the transverse-field ising model, Phys. Rev. A 106, 042426 (2022), doi:10.1103/PhysRevA.106.042426.
- [58] S. Nezami and M. Walter, *Multipartite Entanglement in Stabilizer Tensor Networks*, Phys. Rev. Lett. **125**, 241602 (2020), doi:10.1103/PhysRevLett.125.241602, 1608.02595.
- [59] E. T. Campbell, Catalysis and activation of magic states in fault-tolerant architectures, Physical Review A 83, 032317 (2011), doi:10.1103/PhysRevA.83.032317.
- [60] L. Leone, S. F. E. Oliviero and A. Hamma, Nonstabilizerness determining the hardness of direct fidelity estimation, Phys. Rev. A 107(2), 022429 (2023), doi:10.1103/PhysRevA.107.022429.
- [61] M. Hebenstreit, R. Jozsa et al., All pure fermionic non-gaussian states are magic states for matchgate computations, Physical Review Letters 123(8) (2019), doi:10.1103/physrevlett.123.080503.
- [62] G. Saxena and G. Gour, Quantifying multiqubit magic channels with completely stabilizer-preserving operations, Phys. Rev. A **106**(4), 042422 (2022), doi:10.1103/PhysRevA.106.042422.
- [63] K. Bu, W. Gu and A. Jaffe, Discrete quantum gaussians and central limit theorem, arXiv (2023), [quant-ph/2302.08423].
- [64] C. Weedbrook, S. Pirandola et al., Gaussian quantum information, Reviews of Modern Physics 84(2), 621 (2012), doi:10.1103/RevModPhys.84.621.
- [65] X. Zhang, Z. Pan and G. Liu, Unconditional quantum magic advantage in shallow circuit computation, arXiv (2024), [quant-ph/2402.12246].
- [66] S. Aaronson and D. Gottesman, Improved simulation of stabilizer circuits, Physical Review A 70, 052328 (2004), doi:10.1103/PhysRevA.70.052328.
- [67] D. Gottesman, Stabilizer codes and quantum error correction, arXiv (1997), [quant-ph/quant-ph/9705052].
- [68] R. Jozsa and A. Miyake, *Matchgates and classical simulation of quantum circuits*, Proceedings of the Royal Society A: Mathematical, Physical and Engineering Sciences **464**(2100), 3089–3106 (2008), doi:10.1098/rspa.2008.0189.
- [69] M. Hebenstreit, R. Jozsa et al., Computational power of matchgates with supplementary resources, Physical Review A 102, 052604 (2020), doi:10.1103/PhysRevA.102.052604.
- [70] S. Bravyi and D. Gosset, Improved Classical Simulation of Quantum Circuits Dominated by Clifford Gates, Physical Review Letters 116, 250501 (2016), doi:10.1103/PhysRevLett.116.250501.
- [71] S. Bravyi, G. Smith and J. A. Smolin, Trading Classical and Quantum Computational Resources, Physical Review X 6, 021043 (2016), doi:10.1103/PhysRevX.6.021043.
- [72] S. Bravyi, D. Browne et al., Simulation of quantum circuits by low-rank stabilizer decompositions, Quantum 3, 181 (2019), doi:10.22331/q-2019-09-02-181.
- [73] H. Pashayan, J. J. Wallman and S. D. Bartlett, Estimating outcome probabilities of

- quantum circuits using quasiprobabilities, Phys. Rev. Lett. **115**, 070501 (2015), doi:10.1103/PhysRevLett.115.070501.
- [74] E. Tirrito, P. Sonya Tarabunga et al., Quantifying non-stabilizerness through entanglement spectrum flatness, arXiv e-prints arXiv:2304.01175 (2023), doi:10.48550/arXiv.2304.01175, 2304.01175.
- [75] X. Dong, Holographic Rényi Entropy at High Energy Density, Phys. Rev. Lett. 122(4), 041602 (2019), doi:10.1103/PhysRevLett.122.041602, 1811.04081.
- [76] L. Leone, S. F. E. Oliviero *et al.*, A complete discussion on the theory of nonstabilizerness (In preparation).
- [77] C. Keeler, W. Munizzi and J. Pollack, Entropic lens on stabilizer states, Phys. Rev. A 106(6), 062418 (2022), doi:10.1103/PhysRevA.106.062418, 2204.07593.
- [78] C. Keeler, W. Munizzi and J. Pollack, Clifford Orbits from Cayley Graph Quotients (2023), 2306.01043.
- [79] W. Munizzi and H. J. Schnitzer, Entropy cones and entanglement evolution for Dicke states, Phys. Rev. A 109(1), 012405 (2024), doi:10.1103/PhysRevA.109.012405, 2306.13146.
- [80] C. Keeler, W. Munizzi and J. Pollack, Bounding Entanglement Entropy with Contracted Graphs (2023), 2310.19874.
- [81] M. Jafarzadeh, Y.-D. Wu et al., Randomized benchmarking for qudit Clifford gates, New J. Phys. **22**(6), 063014 (2020), doi:10.1088/1367-2630/ab8ab1.
- [82] D. Gottesman, The Heisenberg Representation of Quantum Computers, arxiv, doi:10.48550/arXiv.quant-ph/9807006 (1998), [Arxiv:quant-ph/9807006].
- [83] M. A. Nielsen and I. L. Chuang, Quantum Computation and Quantum Information, Cambridge University Press (2000).
- [84] E. H. Lieb and M. B. Ruskai, A fundamental property of quantum-mechanical entropy, Phys. Rev. Lett. **30**, 434 (1973), doi:10.1103/PhysRevLett.30.434.
- [85] S. T. Flammia, A. Hamma et al., Topological Entanglement Rényi Entropy and Reduced Density Matrix Structure, Physical Review Letters 103, 261601 (2009), doi:10.1103/PhysRevLett.103.261601.
- [86] X. Dong, The gravity dual of Rényi entropy, Nature Communications 7, 12472 (2016), doi:10.1038/ncomms12472, 1601.06788.
- [87] H. Yao and X.-L. Qi, Entanglement entropy and entanglement spectrum of the kitaev model, Phys. Rev. Lett. 105, 080501 (2010), doi:10.1103/PhysRevLett.105.080501.
- [88] J. Schliemann, Entanglement spectrum and entanglement thermodynamics of quantum hall bilayers at $\nu=1$, Phys. Rev. B **83**, 115322 (2011), doi:10.1103/PhysRevB.83.115322.
- [89] J. de Boer, J. Järvelä and E. Keski-Vakkuri, Aspects of capacity of entanglement, Phys. Rev. D 99, 066012 (2019), doi:10.1103/PhysRevD.99.066012.
- [90] Y. Nakaguchi and T. Nishioka, A holographic proof of Rényi entropic inequalities, JHEP 12, 129 (2016), doi:10.1007/JHEP12(2016)129, 1606.08443.
- [91] P. Bueno, P. A. Cano et al., Universal Feature of Charged Entanglement Entropy, Phys. Rev. Lett. 129(2), 021601 (2022), doi:10.1103/PhysRevLett.129.021601, 2203.04325.

- [92] K. M. Zurek, Snowmass 2021 White Paper: Observational Signatures of Quantum Gravity (2022), 2205.01799.
- [93] N. Bao, C. Cao and V. P. Su, Magic state distillation from entangled states, Physical Review A 105(2) (2022), doi:10.1103/physreva.105.022602.
- [94] P. S. Tarabunga, Critical behaviours of non-stabilizerness in quantum spin chains, arXiv (2023), [quant-ph/2309.00676].
- [95] P. Sonya Tarabunga and C. Castelnovo, Magic in generalized Rokhsar-Kivelson wavefunctions, arXiv e-prints arXiv:2311.08463 (2023), doi:10.48550/arXiv.2311.08463, 2311.08463.
- [96] M. Kim, M.-R. Hwang et al., Average Rényi Entropy of a Subsystem in Random Pure State, arXiv e-prints arXiv:2301.09074 (2023), doi:10.48550/arXiv.2301.09074, 2301.09074.
- [97] C. D. White and J. H. Wilson, *Mana in haar-random states*, arXiv (2020), [quant-ph/2011.13937].
- [98] Z.-W. Liu and A. Winter, Many-body quantum magic, PRX Quantum $\mathbf{3}(2)$ (2022), doi:10.1103/prxquantum.3.020333.
- [99] C. Akers and G. Penington, Leading order corrections to the quantum extremal surface prescription, Journal of High Energy Physics **2021**(4) (2021), doi:10.1007/jhep04(2021)062.
- [100] Y. Ge and J. Eisert, Area laws and efficient descriptions of quantum many-body states, New Journal of Physics 18(8), 083026 (2016), doi:10.1088/1367-2630/18/8/083026.
- [101] J. Molina-Vilaplana, Holographic Geometries of one-dimensional gapped quantum systems from Tensor Network States, JHEP 05, 024 (2013), doi:10.1007/JHEP05(2013)024, 1210.6759.
- [102] A. Anshu, A. W. Harrow and M. Soleimanifar, Entanglement spread area law in gapped ground states, Nature Physics 18(11), 1362–1366 (2022), doi:10.1038/s41567-022-01740-7.
- [103] B. Czech, P. Hayden et al., The information theoretic interpretation of the length of a curve, Journal of High Energy Physics 2015, 157 (2015), doi:10.1007/JHEP06(2015)157, 1410.1540.
- [104] P. Calabrese and A. Lefevre, Entanglement spectrum in one-dimensional systems, Phys.Rev.A 78(3), 032329 (2008), doi:10.1103/PhysRevA.78.032329, 0806.3059.
- [105] P. Hayden and A. Winter, Communication cost of entanglement transformations, Physical Review A 67(1) (2003), doi:10.1103/physreva.67.012326.
- [106] D. D. Blanco, H. Casini et al., Relative entropy and holography, Journal of High Energy Physics 2013(8) (2013), doi:10.1007/jhep08(2013)060.
- [107] T. Faulkner, M. Guica et al., Gravitation from entanglement in holographic cfts, Journal of High Energy Physics 2014(3) (2014), doi:10.1007/jhep03(2014)051.
- [108] B. Swingle and M. V. Raamsdonk, Universality of gravity from entanglement, arXiv (2014), [hep-th/1405.2933].
- [109] S. F. E. Oliviero, L. Leone and A. Hamma, Magic-state resource theory for the ground state of the transverse-field ising model, Phys. Rev. A 106, 042426 (2022), doi:10.1103/PhysRevA.106.042426.
- [110] T. Haug, S. Lee and M. S. Kim, Efficient stabilizer entropies for quantum computers, arxiv, doi:10.48550/arXiv.2305.19152 (2023), [quant-ph/2305.19152].

- [111] P. S. Tarabunga, E. Tirrito et al., Nonstabilizerness via matrix product states in the pauli basis, arXiv (2024), [quant-ph/2401.16498].
- [112] C. Cao, M. J. Gullans et al., Quantum lego expansion pack: Enumerators from tensor networks, arXiv (2023), [quant-ph/2308.05152].
- [113] T. J. Sewell and C. D. White, Mana and thermalization: Probing the feasibility of near-clifford hamiltonian simulation, Phys. Rev. B 106, 125130 (2022), doi:10.1103/PhysRevB.106.125130.
- [114] O. Aharony, J. Marsano et al., The deconfinement and hagedorn phase transitions in weakly coupled large n gauge theories, Comptes Rendus Physique 5(9–10), 945–954 (2004), doi:10.1016/j.crhy.2004.09.012.
- [115] M. Nozaki, T. Numasawa and T. Takayanagi, Holographic Local Quenches and Entanglement Density, JHEP 05, 080 (2013), doi:10.1007/JHEP05(2013)080, 1302.5703.
- [116] P. Caputa, M. Nozaki and T. Takayanagi, Entanglement of local operators in large-N conformal field theories, PTEP **2014**, 093B06 (2014), doi:10.1093/ptep/ptu122, 1405.5946.
- [117] V. Balasubramanian, A. Bernamonti et al., Holographic Thermalization, Phys. Rev. D 84, 026010 (2011), doi:10.1103/PhysRevD.84.026010, 1103.2683.
- [118] T. Hartman and J. Maldacena, Time Evolution of Entanglement Entropy from Black Hole Interiors, JHEP 05, 014 (2013), doi:10.1007/JHEP05(2013)014, 1303.1080.
- [119] C. Akers and P. Rath, *Holographic Renyi Entropy from Quantum Error Correction*, JHEP **05**, 052 (2019), doi:10.1007/JHEP05(2019)052, 1811.05171.
- [120] X. Dong, D. Harlow and D. Marolf, Flat entanglement spectra in fixed-area states of quantum gravity, Journal of High Energy Physics 2019(10) (2019), doi:10.1007/jhep10(2019)240.
- [121] Z. Chen, Z. Ma et al., Sharp continuity bounds for entropy and conditional entropy, Science China Physics, Mechanics & Astronomy 60(2), 020321 (2016), doi:10.1007/s11433-016-0367-x.